



<https://theses.gla.ac.uk/>

Theses Digitisation:

<https://www.gla.ac.uk/myglasgow/research/enlighten/theses/digitisation/>

This is a digitised version of the original print thesis.

Copyright and moral rights for this work are retained by the author

A copy can be downloaded for personal non-commercial research or study,
without prior permission or charge

This work cannot be reproduced or quoted extensively from without first
obtaining permission in writing from the author

The content must not be changed in any way or sold commercially in any
format or medium without the formal permission of the author

When referring to this work, full bibliographic details including the author,
title, awarding institution and date of the thesis must be given

Enlighten: Theses

<https://theses.gla.ac.uk/>
research-enlighten@glasgow.ac.uk

CAVITATION NUCLEI
AND
RESORPTION OF AIR BUBBLES

By

PETER JUI-SHAN CHENG, B.Sc.(Eng.), A.M.I.N.A.

Department of Aeronautics and Fluid Mechanics,

University of Glasgow.

ProQuest Number: 10646853

All rights reserved

INFORMATION TO ALL USERS

The quality of this reproduction is dependent upon the quality of the copy submitted.

In the unlikely event that the author did not send a complete manuscript and there are missing pages, these will be noted. Also, if material had to be removed, a note will indicate the deletion.



ProQuest 10646853

Published by ProQuest LLC (2017). Copyright of the Dissertation is held by the Author.

All rights reserved.

This work is protected against unauthorized copying under Title 17, United States Code
Microform Edition © ProQuest LLC.

ProQuest LLC.
789 East Eisenhower Parkway
P.O. Box 1346
Ann Arbor, MI 48106 – 1346

Thesis
1760
Copy 2



CONTENTS

	Page
Preface	
Acknowledgements	
Part I - Cavitation Nuclei	
1. Introduction	1
2. Model of cavitation nuclei	3
3. Description of apparatus	7
3.1 Test tank	7
3.2 Barium titanate transducer	7
3.3 Mounting of transducer	7
3.4 Reflector	8
3.5 Electronic equipment	8
4. Experimental method and procedure	9
4.1 Aim and scope of experiment	9
4.2 Detection of cavitation onset	9
4.3 Procedures for the determination of the thresholds for gaseous and vaporous cavitation	10
4.4 Deaeration and aeration	12
4.5 Measurement of total air content	13
5. Experimental results and observations	14
5.1 Calibration of sound pressure in the focus of the standing wave	14
5.2 Cavitation thresholds for tap water	16
5.3 Cavitation thresholds for distilled water	22
5.4 Cavitation thresholds for filtered tap water	23
5.5 Effect of wetting agent on thresholds of cavitation	24
5.6 Pressurization	25
6. Variation in experimental conditions and repeatability of results	26
7. Discussion	27
8. Conclusion	31
9. Reference	32
10. List of tables and figures	35

Part II - Resorption of Air Bubbles

List of symbols and values of constants used

1. Introduction	----	----	1
1.1 Aim of the experiment	----	----	3
2. design and description of apparatus	----	----	3
2.1 The main tube	----	----	4
2.2 Pressurization	----	----	4
2.3 Bubble generation	----	----	4
2.4 Measurement of rate of resorption	----	----	4
2.5 Lighting	----	----	5
2.6 Air content of water	----	----	5
3. Experimental procedure and technique	----	----	6
3.1 Preparation of water	----	----	6
3.2 Setting ambient pressure	----	----	6
3.3 Bubble generation	----	----	7
3.4 Time - distance record	----	----	7
3.5 Range covered by experiment	----	----	8
4. Experimental results	----	----	9
5. Analysis of experimental results	----	----	11
5.1 Lewis-Whitman equation	----	----	11
5.2 Rate of change of bubble radius	----	----	11
5.3 Bubble radius and its rising velocity	----	----	12
5.4 Evaluation of K_L	----	----	14
5.5 Resorption equations for air bubbles	----	----	15
6. Sources of error	----	----	18
7. Discussion	----	----	20
8. Conclusions	----	----	21
9. Reference	----	----	22
10. Appendix	----	----	24
11. List of tables and figures	----	----	26

PREFACE

It has now been generally accepted that the formation of cavities in flowing or static water upon the reduction of local pressure is due to the growth of microscopic gas nuclei to visible size. The sizes of such nuclei determine the inception pressure of cavitation. In water tunnels where model testing are carried out to predict the inception point of a prototype it is necessary to learn more about the characteristics of the nuclei present in the tunnel water and the water used in the prototype before a proper scaling law may be derived.

The air bubbles formed by cavitation in the working section of the water tunnel make the prolonged operation of tunnel unsatisfactory if not removed. Resorbers have been constructed to force these free air bubbles back into solution. The dimension of the resorbers was determined by using the resorption equations for air bubble in undersaturated water based on the Lewis-Whitman concept of gas and liquid films. The empirical liquid coefficient K_L is of direct importance in fixing the dimension of the resorber.

The thesis is divided into two parts. The first part describes the investigation into the characteristics of nuclei commonly present in water and the possible mechanisms of stabilization of such nuclei. In part two, an apparatus is described for evaluating the empirical liquid coefficient K_L for small air bubbles.

ACKNOWLEDGEMENTS

The work was carried out in the University of Glasgow under the guidance of Professor W. J. Duncan.

The author wishes to acknowledge his indebtedness to Professor W. J. Duncan and Mr. P. H. Tanner for their support of the work and their guidance and encouragement during the investigation.

His gratitude is also due to the Electrical Engineering Department for the loan of electronic equipment and to Mr. A. W. Connell for the valuable help and advice rendered on various matters concerning electronics.

For the work shop staff he wishes to express his thanks for their co-ordination and their skill in making part of the apparatus.

He finally wishes to thank the superintendent of Fluids Division, Mechanical Engineering Research Laboratory for the use of their library and the loan of the Air Content Apparatus.

(PART I)

CAVITATION NUCLEI

CAVITATION NUCLEI.

1. Introduction

The formation of cavities in water under reduced pressure was first observed by Reynolds (ref.1) in a venturi, but its engineering implication was only realised in connection with the design of high speed marine propellers. Barnaby (ref.2) explained that the decrease in efficiency of marine propellers at high speed was due to the formation of cavities on the back of the propeller blades filled with water vapour and air. This explanation was borne out by Parson's experiment (ref.3) on a model propeller in a heated water tank under reduced pressure. R.E. Froude suggested that this phenomenon be described by the term "Cavitation."

Since then much work has been done on the subject; for the background of the general aspects of cavitation references 4 to 7 should be consulted.

One basic problem which is of interest to both scientists and engineers is the determination of the critical pressure for the onset of cavitation in a liquid. To the physicist this represents the maximum negative static pressure (tension) the liquid will stand, i.e., the tensile strength of the liquid, while to the hydrodynamicist the dynamic inception pressure is the criterion for cavitation free operation in hydrodynamic machines such as ship propellers. More recently the interest was shared by the acoustical engineers concerned with the transmission of sound waves in liquids and the process of ultrasonic cleaning.

A review of the literature such as that by Temperley and Chambers (ref.8) shows that the reported values of the tensile strengths of liquids are widely scattered. It is now known that this is due to the different experimental methods used, the effect of air and solid particle contents and the effect of pre-treatment of the specimens.

In the field of hydrodynamics it had long been assumed that flowing water could not withstand tension and vapour cavities would form in water when the pressure was reduced to that of the vapour pressure corresponding to the water temperature. It is now realized that cavitation may occur above or below vapour pressure depending on the condition of the water.

Quantitative measurements of the threshold for ultrasonic cavitation in water have only recently been undertaken. (ref.9 to 13) The results show large differences between measurement by different workers.

It has now been generally accepted that the discrepancies between the various values of critical pressure for the inception of cavitation in water are due to the presence of weak spots in water. These weak spots have been given the name "nuclei." Experimental evidence has led to speculation that they are cavities containing undissolved air. The first of such experiments was performed by Harvey et al. (ref.14). They showed that by applying a temporary high pressure (1000 atms.) to a water sample the resistance to cavitation was greatly increased. This pressurization effect has since been confirmed by Strasberg (ref.12), Iyengar and Richardson (ref.13) and Knapn (ref.15). It was explained that the high pressure forced the undissolved air cavities into solution and thus removed the nuclei or weak spots in water. Since the sizes of such nuclei probably determine the critical pressures for the onset of cavitation in water, for a better understanding of the mechanism of inception we must try to learn more about the characteristics of the nuclei in water. It was with this aim that the present work was undertaken.

2. Model of Cavitation Nuclei.

2.1 Free Air Bubbles.

In order to explain the ease with which untreated water can be made to cavitate it is necessary to postulate that microscopic gas nuclei (10^{-3} to 10^{-5} cm) exist in water which has not been specially treated. Cavitation is the growth of such nuclei to visible size. It is unlikely that the gas nuclei are free air bubbles, since they will be compressed out of existence by the surface tension or grow by the diffusion of air into the bubble and eventually rise out of the water. Consider the equation of statical equilibrium for an air bubble in water.

$$p_o = p_g + p_v - \frac{2\sigma}{r} \dots\dots\dots (2.1.1)$$

where p_o = water pressure.

p_g = gas pressure in bubble.

p_v = vapour pressure

σ = surface tension

r @ radius of bubble.

The equilibrium can only be maintained if

$$p_g = p_L \dots\dots\dots (2.1.2)$$

where p_L is the equivalent dissolved gas pressure. Therefore in saturated or supersaturated water there is only one size of bubble which can maintain the equilibrium. Larger bubbles will grow by the diffusion of air into the bubble and smaller ones will dissolve under the pressure of surface tension. In undersaturated water all bubbles will soon dissolve. Experimental evidence showed that nuclei persisted even in undersaturated water. Therefore some mechanism must exist which stabilizes the gas nuclei and prevents their absorption in undersaturated water.

Before going on to examine the possible mechanisms of stabilization we shall assume that free air bubbles exist in water and the condition under which they will grow can be calculated.

From equation (2.1.1) it had been shown by Blake (ref 9) and also by Neppiras and Noltingk (ref.20) that there is a limit to the mechanical stability of such a bubble. The minimum pressure p_o at which the bubble become unstable is given by the equation.

$$p_c = p_v - \frac{8}{9} \left[\frac{3}{2} \frac{\sigma^3}{r_o^3 (p_o + \frac{2\sigma}{r_o})} \right]^{1/2} \dots\dots\dots(2.1.3)$$

where r_o = initial radius of bubble

p_o = initial hydrostatic pressure outside bubble.

Equation (2.1.3) gives the critical pressure for the occurrence of vaporous cavitation.

The bubble can also grow by the diffusion of air into the bubble if it is subjected to a forced oscillation by a sound wave (ref 9 and ref 21). During the positive half-cycle the air inside the bubble is compressed and diffuses out of the bubble, but during the negative half-cycle the air diffuses into the bubble from the surrounding water. Since the expanded surface area in the negative half-cycle is larger than the contracted surface area in the positive half, there is a net influx of gas into the bubble. If this influx is greater than the amount of gas dissolved, in the same time, the bubble will grow. Therefore there is a threshold for the growth of bubbles by induced sonic oscillation depending on the air content of water, the hydrostatic pressure, radius of the bubble and the frequency of the sound wave. The peak sound pressure p_s required to cause gaseous cavitation is given by Blake (ref 9) as,

$$p_s = 6^{1/2} p_o \frac{[1 + 4\sigma/3r_o p_o] [1 + 2\sigma/r_o p_o - \frac{p_L}{p_o}]^{1/2}}{[1 + (2\sigma/r_o p_o)]^{1/2} [1 + 2r_o (\frac{f}{2D})^{1/2}]^{1/2}} \dots\dots\dots(2.1.4)$$

where f = frequency of sound wave

D @ diffusivity

Without questioning the mechanism of stabilization and by assuming the existence of a microscopic gas nuclei (spherical) it is possible to derive the peak sound pressure required for vaporous and gaseous cavitation. The critical pressure p_c is equal to $(p_s - p_o)$.

Two theories exist to explain the persistence of the gas nuclei in undersaturated water.

2.2 Gas nuclei with organic skin.

A hypothesis was put forward by Fox and Herzfeld (ref.22) to

explain the persistence of nuclei in water. They suggested that gas nuclei are stabilized by an organic skin which covers the whole bubble. As air diffuses out of the bubble the size of the bubble will be reduced and the skin compressed. The compression of the skin finally cuts off the solution of more air and diffusion ceases. Alternatively the skin acts as an elastic shell to support the pressure difference between the gas pressure, pressure due to surface tension and the water pressure. This allows the air inside the bubble to reach diffusion equilibrium with the dissolved air in water even if it is undersaturated.

As shown in reference (22) the maximum size of bubble which will survive under a ^{max.} hydrostatic pressure of p_m will have a radius.

$$r_m = \frac{2(C_s - \sigma)}{p_m - p_L} \dots \dots \dots (2.2.1)$$

where C_s - crumpling strength of the skin. The gas pressure inside the bubble is assumed to be equal to the equivalent dissolved gas pressure.

The peak sound pressure required to cause vaporous cavitation is given by reference (22) as

$$p_s = p_o - p_L + 2(T_s + \sigma) \left(\frac{1}{r} + \frac{1}{a'} \right) \dots \dots \dots (2.2.2)$$

where T_s - tensile strength of the skin

a' - a constant

If r_m is used in equation (2.2.2) we have,

$$p_s = p_o + A p_m - (1+A) p_L + B \dots \dots \dots (2.2.3)$$

where $A = \frac{T_s - \sigma}{C_s + \sigma}$ and $B = \frac{2(T_s + \sigma)}{a'}$

2.3 Air trapped in a crevice.

The concept of undissolved air trapped in the unwetted crevice of suspended particles as the model of nuclei was due to Harvey (ref.14). If the wall of the crevice is hydrophobic the liquid /air surface will be convex towards the air if the water is undersaturated and the surface tension force will act opposite to that of water pressure.

The air pressure inside the crevice can be kept in diffusion equilibrium even if the water is undersaturated.

The peak sound pressure for vaporous cavitation was calculated by Strasberg (ref.12) as

$$p_s = p_o + B_o p_m - (B_o + B_1) p_L \dots \dots \dots (2.3.1)$$

where B_o and B_1 are numerical constants depending on the geometry of the crevice and the receding angle of contact and the solid/gas/liquid interface.

Strasberg (ref.12) observed that with two completely different concepts of the mechanism of stabilization of the nuclei the critical pressures for vaporous cavitation show a similar linear relationship with p_m and p_L . This renders the verification of the mechanism of stabilization by experiment more difficult.

3. Description of apparatus

The apparatus is similar to that used by Iyengar and Richardson (ref.13) with differences in the details of construction. The sound pressure to cause cavitation is generated by setting up a spherical standing wave system in a test tank with a barium titanate bowl transducer and reflector. With this system high sound pressures can be generated in the body of the liquid away from any solid surfaces. The properties measured are therefore those of the liquid tested. A general view of the apparatus used is shown in Fig (1).

3.1 Test Tank.

The tank was constructed of perspex sheet. The main dimensions are given in Fig (2). The top and bottom covers of the tank were removable and were bolted to the flanges on the side of the tank using rubber gaskets. Drain holes were provided on the top and bottom covers. Water for testing was drawn into the tank through a rubber tube connected to the bottom drain hole to avoid splashing and air entrainment. Fig (3) shows the test tank together with the barium titanate transducer and reflector in place.

3.2 Barium Titanate transducer

The spherical transducer was made to order by Technical Ceramic Limited. It had a radius of curvature of 6.35 cm. and a uniform thickness of 6 m.m. The diameter across the face of the transducer was 10.6 cm. Both sides of the transducer were silver plated and electric contact was made by means of spring contacts. (see fig.2)

3.3 Mounting of transducer.

The mounting for the transducer was made of two Bakelite discs. It was designed to reduce the restraint on the transducer to a minimum. The transducer was clamped around its perimeter along the centre of the thickness by means of a rubber "O" ring and the "V" groove cut on the two discs, since the centre of the thickness was a node

when the transducer was driven at half-wave resonance.

The mounting together with the transducer was bolted to one end of the tank with rubber gasket as shown in Fig (2). The transducer thus had air backing (high potential side) and was in direct contact with the liquid under test inside the tank (ground side).

3.4 Reflector

The reflector was also made of perspex. The surface shell facing the transducer was made of $\frac{1}{16}$ " thick perspex sheets and had the same radius of curvature as the transducer. The spherical shape was obtained by pressing the heated perspex sheet into a mould and polishing to the required finish. The spherical shell was then glued to the base around its perimeter leaving an air space between the shell and the base. The use of perspex for the construction of the reflector facilitated the lighting of the tank. Coarse focusing of the reflector was effected by shifting the perspex shaft on which it was mounted. An adjusting nut on the shaft provided the fine movement needed for focusing.

3.5 Electronic equipment .

A block diagram of the electronic equipment used is given in Fig (4). The spherical transducer was driven at its resonant frequency of 428kc/sec through a tuned L C circuit by a modified T10 radio transmitter. The transmitter was supplied by Siemens Edison Swan Ltd. The power output was controlled by varying the E.H.T. of the power amplifier. A Marconi valve voltmeter was used to measure the voltage applied to the transducer. For a standing wave the maximum voltage available to drive the transducer was 80 volts and corresponded to a peak sound pressure of 30 atmospheres at the focus of the standing wave.

The sound pressure at the focus of the standing wave was measured by a ultrasonic probe UP800C also supplied by Technical Ceramic Ltd., whose sensitive element was $\frac{1}{16}$ " in length and 0.058" in diameter. The accuracy quoted by the maker was ± 2 db.

4. Experimental method and procedure

4.1 Aim and Scope of experiment.

The aim of the experiment was to determine the cavitation thresholds of tap water, distiller water and filtered tap water under various experimental conditions and to deduce from the results, the characteristics and the mechanism of stabilization of gas nuclei.

The majority of the experiments were conducted on tap water. For the purpose of comparison some experiments were repeated in distilled water and one in filtered tap water.

The thresholds of gaseous and vaporous cavitation were determined in many samples and the effects of such factors as age of water, total air content, re-aeration and deaeration, wetting agent and pressurization on the thresholds were investigated.

4.2 Detection of Cavitation onset

The onset of cavitation in water for both gaseous and vaporous cavitation were detected by the resulting noise. The spherical transducer was used also as a detector and the noise was made visible by feeding the signals received into an oscilloscope. A twin - T filter was used to eliminate the driving signal of 428 kc/sec so that only the noise generated by bubbles were displayed on the screen of the oscilloscope. However a small portion of the r.f. signal still appeared on the screen, but since the amplitude of this residual signal was comparable to that of the noise generated by the bubbles at onset of cavitation, which were also of a much lower frequency, there was no difficulty in distinguishing one from the other. No attempt was therefore made to improve the filter used.

The noise generated by gaseous cavitation had a broad frequency range and was continuous while the noise caused by vaporous cavitation appeared as individual pulses having by rough estimation a duration less than one milli second.

This method of detection is similar in principle to the method used by Iyengar and Richardson (ref.4) and has many advantages over visual detection.

For gaseous cavitation in air saturated water the onset of noise was accompanied by the sudden appearance of small bubbles in the focal region. However for partially degassed water ($>50\%$ saturation) the noise sometimes appeared long before any bubbles became visible, and if the appearance of bubbles had been taken as a criterion for the onset of gaseous cavitation the threshold would have been overestimated. Since the onset of gaseous cavitation is identified with a the growth of a bubble by a process called "rectified diffusion" the threshold should be defined as the pressure which will cause the growth by this process irrespective of the time required for the bubble to grow to a certain size.

At the frequency of 428 kc/sec the bubbles generated by vaporous cavitation never grew to visible size before their final collapse at a sound pressure slightly higher than the threshold. It was therefore not possible to determine the threshold of vaporous cavitation by visual inspection in the present experiment. It is to be noted that at sound pressures very much higher than the threshold for vaporous cavitation the vapour bubbles generated by cavitation did become visible to unaid eyes.

4.3 Procedures for the determination of the thresholds of gaseous and vaporous cavitation.

To determine the thresholds of gaseous and vaporous cavitation it was found necessary to adopt a different procedure for each. To determine the threshold of gaseous cavitation in water the sound pressure was increased slowly until noise appeared on the oscilloscope indicating the onset of gaseous cavitation. The appearance of noise might or might not be accompanied by the appearance of bubbles depending on the total air content of the water. The voltage applied to the transducer was noted and the sound wave was turned off immediately to prevent further formation of bubbles. Unlike the apparatus used by Strasberg (ref.12) where only one bubble was formed the present apparatus continued

to produce bubbles if the sound wave was left on.

When all the bubbles produced had risen to the top of the tank and none could be seen in the body of the water, especially in the focal region, the water was slightly stirred with the polythene tube stirrer. Experience showed that if the second measurement was undertaken without replacing the water in the focal region which had been subjected to cavitation, the threshold determined was in many cases either higher or lower than the first measurement. Results showed that more consistent readings were obtained if fresh water was brought into the focal region after each measurement.

About thirty seconds after the water was stirred the second measurement was made. This time the sound pressure was quickly brought up to a point about 10% below the threshold measured in the first trial. If no cavitation occurred before this point was reached the sound pressure was held there for ten seconds. And if no cavitation occurred during that time the sound pressure was increased in steps every ten seconds until the threshold was reached. By bringing up the sound pressure quickly to the neighbourhood of the threshold estimated by the first trial it was hoped to reduce the time effect and to limit the heating of the water in the focal region to a minimum. This was repeated six to eight times, and the arithmetical mean of the measurements obtained was taken to be the threshold of the water tested.

The procedure adopted for determining the threshold of vaporous cavitation was slightly different from that for gaseous cavitation. It was realised that at a low total air content where most of the experiments for vaporous cavitation were carried out the nuclei available for cavitation are few in number. In order to derive a threshold which is representative of the whole body of the water the following procedure was used. As in the procedure for gaseous cavitation the first measurement was

used to estimate the approximate value of the threshold. When that was determined the water was slightly stirred and thirty seconds were allowed to elapse before the sound pressure was again increased to a point 10% below the estimated threshold. During the increase a close watch was kept on the screen of the oscilloscope to see whether any vaporous cavitation took place. If a pulse was seen on the screen the lower value was to be taken as the estimated threshold and the sound pressure brought to a point 10% below that. The sound pressure was then held there for ten seconds. If no cavitation was detected during that time the sound pressure was turned off and the water slightly stirred. Thirty seconds later the sound pressure was again brought up to the same value for ten seconds. This was repeated for five times. If no cavitation occurred during that time the sound pressure was then increased and the procedure repeated until vaporous cavitation did occur at least once during the five trials. In order to establish that this was not due to an extra weak nucleus the procedure was repeated another ten times and the pressure was taken to be the threshold of vaporous cavitation if at least 5 of the ten trials resulted in a vaporous cavitation. Admittedly the threshold determined in this way was arbitrary in nature but it did represent a threshold which was most representative of the whole body of water tested. This procedure also limited the sound radiation to ten seconds each time and the effect of heating will be very small.

4.4 Deaeration and re-aeration

Deaeration of water samples was accomplished by shaking the glass bottle containing the sample under vacuum. When the desired air content was approximately reached the water was then transferred to the test tank. Care was taken not to cause any splashing of the water when it was drawn into the tank through the bottom drain hole.

Water was allowed to fill the whole tank and any air bubbles trapped in the tank were removed by tilting the tank and causing them to escape through the overflow. A polythene tube was then inserted into the tank through the overflow to serve as a stirrer as well as helping to keep the air content of water nearly constant over a long period.

Re-aeration of degassed samples was carried out in these ways.

(1) The degassed sample was allowed to stand quietly in a polythene bottle under atmospheric pressure. The bottle was closed to avoid the collection of dust on the water surface. The restoration of air content was by the slow process of molecular diffusion.

(2) The air content was restored by mixing the degassed sample with water saturated with air. The resultant air content depended on the amount of saturated water added.

(3) The air content of a degassed sample was restored by bubbling air through it. The arrangement is shown in fig (5). The vacuum pump was used to provide the suction required to draw air into the bottle. The rate of flow of air was controlled by the glass stop cock. By this method there was no fear of oil contamination (commonly present in compressed air) and no filter was required.

4.5 Measurement of total air content.

The measurement of the total air content was made by the M.E.R.L. air content apparatus (ref.17) using the corrections suggested by Kaneillopoulos (ref.18 & 19) The measurement of the air content was always carried out after the determination of the threshold.

5. Experimental results and observations.

5.1 Calibration of sound pressure in the focus of the standing wave.

To measure the sound pressure in the focus of the standing wave an Ultrasonic Probe UP 800C was obtained from Technical Ceramics Ltd. To convert the output voltage of the probe to sound pressure a calibration curve was supplied by the manufacturer with five points covering the frequency range from 20kc/sec to 1Mc/sec.

It was not practical to use the probe directly in measuring the pressure at which cavitation occurred during an experiment. Since the presence of the probe in the sound focus would cause cavitation to occur on the body of the probe first. It was decided to use the voltage across the transducer as a measure of the sound pressure at the focus of the standing wave. With the probe placed in the focus of the standing wave the voltage across the transducer was calibrated against the output voltage of the probe which in turn was converted to sound pressure by using the manufacturer's calibration curves.

One difficulty immediately presented itself. In the present system the standing wave was established by using a spherical transducer and reflector. The reflector was placed at a distance away from the transducer approximately equal to twice the radius of curvature of the transducer. The voltage across the transducer was the vector sum of the driving voltage and the voltage induced by the reflected sound wave. The phase difference between the two components depended on the distance of the reflector from the transducer, the frequency of the sound wave and the velocity of sound in water. If the velocity of sound remained constant at a fixed frequency a position would be found for the reflector so that the two components were in phase resulting in a maximum available pressure in the focus as well as a maximum voltage across the transducer for a given amount of electric power applied. Unfortunately the temperature of the water used varied from 11°C to 16°C during an experiment which might last for 1 to 2 days. The change in the velocity of sound is 1.3% for a temperature difference of 5°C. From the equation.

$$c = f \cdot l \dots \dots \dots (5.1)$$

where c - velocity of sound
f - frequency
l - wave length.

for a constant frequency the variation in wave length will also be

1.3%

The distance between the transducer and reflector was approximately 120 mm, the accumulated increase of wave length over that distance was 1.56 mm which is nearly half a wave length at 428 kc/sec (3.4 m.m.) Hence a variation in the temperature of the water used resulted in a shift of phase between the two components of the sound waves, and the sound pressure in the focus of the standing wave might not vary in the same proportion as the voltage across the transducer for a given temperature variation. A calibration of sound pressure against the voltage across the transducer at one temperature could not be useful for any other temperatures.

To overcome this difficulty two methods can be used.

(1) To change the frequency slightly so that the wave length λ remains constant as the temperature varies.

(2) To take up the accumulated increase in wave length by shifting the reflector accordingly.

The first method was not practical under the present system. The transmitter employed to drive the transducer had a tuned master oscillator, a tuned power amplifier and a tuned LC circuit. To tune the frequency as the temperature varies before each measurement will be most elaborate.

The second method was therefore used. An adjusting nut was provided for the fine movement of the reflector (see fig.2). As the temperature varied the reflector was moved accordingly by turning the adjusting nut with the sound wave turned on at low power until the voltage across the transducer reached a maximum, indicating that the components were in phase.

In order to establish that moving the reflector is an adequate remedy for this temperature effect, calibration of the sound pressure against the voltage across the transducer was carried out at seven different temperatures. The temperature of water was increased by heating it with two 150 watts incandescent lamp.

The results are tabulated in table (1). It indicates that the system adopted was adequate. The mean values were used for plotting the calibration curve in fig (6). Fig(6A) demonstrates the shift of phase between the two components as the temperature varies. The components were in phase at 10°C and the voltage across the transducer was 2 volts. It shows that the phase of sound pressure in the focus varies with that of the voltage across the transducer but their amplitude are not in the same proportion.

The dotted line shown in fig (6) is the calibration curve for progressive wave, the reflector being removed in the case. On comparison with the standing wave it shows that the pressure in the focus was approximately the same for the same voltage across the transducer since in a standing wave the pressure in the focus was doubled for a given power input but the voltage across the transducer was also doubled (due to induced voltage) in the present system with the result that for the same voltage across the transducer the pressure in the focus was the same for the progressive and standing waves. For a given power input the maximum available pressure was doubled in the later compared with the former case.

As shown in Fig (6) the pressure at the focus in the standing wave was actually less than that of the corresponding progressive wave for the same voltage. This was to be expected, since the alignment of the reflector was by no means perfect resulting in the slight reduction of pressure in the focus of the standing wave.

5.2 Cavitation thresholds for tap water.

In reported experiments on tap water (ref.12 & 13) water samples were drawn into the tank directly from the tap resulting in the entrainment of numerous small air bubbles. There is reason to believe that this way of drawing water has some effect on the threshold. To understand the behavior of tap water we must investigate the past history of the water.

The source of tap water varies in different places. For most cases water is drawn from a lake or reservoir where the temperature is usually much lower than room temperature and for this reason the tap water is always supersaturated

with air at room temperature. After passing through filter beds where most of the suspended solids are removed the water there enters the mains. Since the pressure in the mains is much higher than atmospheric pressure all tap water has been pressurised to a certain extent.

It is with these points in mind that the first experiment was undertaken.

Water was drawn from the tap in two different ways

(1) Water was drawn with the tap running free, resulting in a cloud of entrained air bubbles. The threshold of cavitation was determined when no visible bubbles could be seen in the body of the water. The cavitation was gaseous in this case.

(2) With a tube connected directly to the tap water was drawn out slowly into the tank through the bottom drain hole. Care was taken not to cause any splashing. Under strong light it could be seen that there were no minute bubbles in the water.

One test immediately followed the other so that the same batch of water was used in the two experiments. The experiment was repeated on six different days and the peak sound pressures which caused cavitation are listed in table (2). In each case the peak sound pressure is higher if the tap water is drawn out quietly.

5.2.1 Ageing of tap water.

Strasberg (ref.12) observed that if freshly drawn tap water is left standing for several days the threshold increases gradually from $\frac{1}{2}$ atmosphere to $1\frac{1}{2}$ atmospheres. He explained this by saying that it is most probably due to the rising of very small bubbles out of water. The magnitude of the time involved is of the right order, if we assume that bubbles of the size 10^{-4} to 10^{-5} can exist in water. Stoke's Law is used to calculate the velocity of rise of such small bubbles. This relationship was used by Iyengar and Richardson (ref.13) to determine the sizes of nuclei in water, although in their experiments the time involved was only seven hours for the threshold to increase from 1.75 atmospheres to 4 atmospheres.

In view of these experimental results, one of the present experiments was designed to investigate further the mechanism of ageing of tap water. On the assumption that the increase in threshold with time is due to the rising of microscopic bubbles then the time required for a certain size of bubble to rise out of water is proportional to the depth of the water below the sound focus. On changing the depth of water below the sound focus the ageing curve of the tap water should also shift along the time axis.

The test tank as described in section (3.1) had removable end covers and extensions could be easily connected to it to increase the depth of water below the sound focus. However experiments with freshly drawn tap water (free running tap) standing in the tank showed no perceptible increase in threshold with time and the investigation was thus abandoned.

Altogether six samples were investigated. The results are tabulated in table (3). In each case water was drawn from the tap into a large glass bottle, transported to the test tank and drawn into the tank through the bottom. An air space was left between the tank top cover and the water surface to allow water to attain saturation condition while standing. The first measurement was taken when the water had been standing for 15 minutes. By that time there were be no visible bubbles in the body of the water. Each value listed in table (3) is the arithmetical mean of six to eight measurements. No trend can be observed in the results.

5.2.2 Effect of total air content on the thresholds of cavitation.

Even without any quantitative measurements much can be learned about the effect of air content on the threshold of cavitation. For quietly drawn tap water (supersaturated with air) minute bubbles suddenly appeared in the focus as the threshold for gaseous cavitation was reached and the cavitation zone quickly spread to both sides of the focus. The motion of the bubbles was similar to those observed by Blake (ref.9),

Strasberg (ref.12) and Iyengar and Richardson (ref.13).

There is no intention of repeating the detail description and only such details which may be of interest are recorded.

The bubbles were observed to appear one by one at a pressure antinode and each one moved along exactly the same circular path to a pressure node where they coalesced to form a large bubble. This large bubble remained trapped at the pressure antinode until it grew to such a size that buoyancy force finally overcame the sound force and it rose to the top of the tank. These circular paths along which the bubbles travelled were spread at half a wave length apart and their planes were perpendicular to the axis of the transducer. From the side of the tank they appeared as evenly spaced rings increasing in diameter with distance from the focus. The spreading of the cavitation zone to both sides of the focus, only happened in the case when the water was near saturation and the peak sound pressure to cause cavitation was higher than $1\frac{1}{2}$ atmosphere. At lower air contents or if the peak sound pressure to cause cavitation was lower than $1\frac{1}{2}$ atmospheres in saturated water, the bubbles only appeared in the focal region at the threshold and there was no tendency for the cavitation zone to spread if the sound pressure was kept constant.

When the total air content was reduced to about 50% saturation gaseous cavitation gave way to vaporous cavitation in tap water. The transition from one to the other was not very clearly defined. A region existed where the two forms of cavitation occurred either separately or simultaneously. On further reducing the air content the vaporous cavitation became predominant and always was the first to appear. But if the sound pressure was increased beyond the threshold for vaporous cavitation the familiar noise of gaseous cavitation could also be seen among the pulses generated by the vaporous cavitation. There was a lower limit of air content beyond which no gaseous cavitation could be

initiated however high the sound pressure.

The effect of total air content on the thresholds of gaseous and vaporous cavitation were determined by changing the air content of the same sample. No attempt was made to determine the threshold of vaporous cavitation at high air content (>50% saturation) although vaporous cavitation could also be initiated by raising the sound pressure beyond that for gaseous cavitation. The swarm of bubbles produced by gaseous cavitation would have affected the sound pressure in the focus and thus made the measurement unrealistic.

5.2.3 Effect of deaeration on the thresholds of cavitation.

After the tap water had been standing in the tank for several days during which time the effect of age on threshold of cavitation was determined the sample was then degassed in stages to determine the effect of deaeration on the thresholds. After each stage of deaeration the sample was allowed to stand for 15 minutes before any measurements were made. Experience showed that after the sample had been subjected to the low pressure of the vacuum pump it took some time for the equilibrium condition to be re-established. After each experiment a sample was drawn and its air content determined.

The experimental results are shown in fig (7) and fig (8).

There are a few points in the experimental results worth noting.

(1) The scatter is quite large for the six samples of tap water, but on close examination it will be noted that if the results of only one of the samples are used, the spots seem to lie on well defined **curves** for both gaseous and vaporous cavitation. Therefore there is reason to believe that tap water drawn on different days (over a period of three weeks for the present experiment) under identical conditions may not have the same threshold for cavitation. In other words the content or sizes of nuclei may be different.

(2) The encircled spots on the extreme right of fig (7) represent the threshold for gaseous cavitation before deaeration. It is to be noted that on the first stage of deaeration the air content was reduced from approximately 22 c.c./litre water to 19.5 c.c./litre water, but no increase in the threshold was noted. In one case the threshold decreased.

In view of these experimental results it was decided to carry out the rest of the experiment by using the same batch of water in the hope that this would give more consistent results than by using water drawn on different days. Water drawn from the tap was allowed to stand in a large storage tank for 10 days. The tank was covered to prevent the collection of dust.

The experiments on the effect of deaeration on the thresholds of cavitation were repeated on the water drawn from the tank. Fig (9) and fig (10) show the results for six samples of water.

It can be seen that by using the same batch of water the results become more consistent and the threshold for both vaporous and gaseous cavitation varies as a linear function of the total air content within their own region of predominance. On superimposing fig (7) and fig (8) on fig (9) and fig (10) respectively it will be noticed that for gaseous cavitation the average values of the threshold for water from different batches lie very close to that for water from the same batch. For vaporous cavitation the threshold for water from the same batch seems to form the upper limit for that of different batches.

5.2.4 Effect of re-aeration on the thresholds of cavitation.

The re-aeration of degassed tap water was accomplished in three ways as stated in section (4.4). The same sample which was used for the experiment on deaeration was used for re-aeration.

Re-aeration by mixing with saturated water.

When the deaeration experiment on one sample was completed, the degassed water was withdrawn from the tank and a pre-determined amount of saturated water added. The threshold was again determined and the resultant air content measured. More saturated water was then added and the process repeated.

Re-aeration by bubbling air through degassed water.

With the arrangement shown in fig (5) air was drawn through degassed tap water and the threshold and air content were determined.

Re-aeration by standing.

Degassed tap water was allowed to regain its air content by standing in a large polythene bottle. The threshold and air content were determined every 12 hours. The water was always thoroughly stirred and allowed to mix properly before any measurement was taken. This eliminated local concentration of dissolved air.

The results for the above experiments are shown in fig (11). Two degassed samples were used for the re-aeration by mixing, but only one each was used for the re-aeration by bubbling and by standing. The remaining water in the storage tank unfortunately was thrown out by mistake before any more experiments could be made.

From fig (11) it can be seen that re-aeration by either bubbling or mixing resulted in a threshold very near to the original value. But in the case where air content was restored by quiet molecular diffusion a hysteresis effect seems to exist.

5.3 Cavitation thresholds for distilled water.

For the purpose of comparison a number of experiments were repeated in distilled water. The results of the experiments are shown in Fig (12 and 13).

5.3.1 Effect of deaeration on threshold of cavitation.

Saturated distilled water cavitated at a critical pressure of about - 2 atmospheres (3 atmospheres peak sound pressure). The cavitation might be gaseous or vaporous. If vaporous cavitation appeared first it was always followed

immediately by gaseous cavitation although the reverse was not always true. There is reason to believe that the transition from gaseous to vaporous cavitation took place in the neighbourhood of - 2 atmospheres critical pressure for distilled water. Although the cavitation was not exclusively vaporous these points are included in fig (13) and marked with a circle round them. At lower air contents the vaporous cavitation always appeared first. For air content above 50% saturation (approximate) gaseous cavitation always followed the first vaporous burst. The air content below which no gaseous cavitation could be initiated appeared to be approximately the same as that for tap water.

As expected the threshold for vaporous cavitation is much higher in distilled water than in tap water for the same air content.

5.3.2 Effect of re-aeration on the thresholds of cavitation.

Four samples were re-aerated. The results are shown in fig (12). When re-aerated by bubbling air through it the threshold approached that of tap water as the air content was increased and the appearance of cavitation also changed from vaporous to gaseous. No hysteresis effect was shown by the samples re-aerated by standing. The threshold was slightly lower in both samples.

5.4 Cavitation thresholds for filtered tap water.

The above experiment indicates that dust particles play a major part in determining the thresholds of cavitation. It was reasoned that if dust particles are removed from the tap water there should be a noticeable increase in the threshold.

Tap water from the storage tank was filtered through a glass filter with pore diameter ranging from 60-100 microns. Only one sample was de-aerated and tested. The result is shown in fig (13). The removal of dust particles or suspended solids increases the cavitation threshold of tap water to nearly that of distilled water. Letters in brackets beside the experimental points indicate the nature of cavitation.

5.5 Effect of wetting agent on threshold of cavitation.

The experimental evidence indicated that the nuclei in water were suspended dust particles. It was thought that the addition of wetting agent to the water should increase the threshold.

3 c.c "Johnson's 326" wetting agent per litre of water was added to each sample. The addition of wetting agent had a marked effect on the threshold and appearance of cavitation. Some observations are described in detail.

When wetting agent was added to saturated tap water a number of small bubbles ($r \sim 3 \times 10^{-3}$ cm) was seen to rise in the body of the water. The origin of the bubbles is not clear. Another interesting phenomenon was noted when gaseous cavitation was initiated in saturated tap water after the addition of wetting agent. As in untreated tap water, minute bubbles appeared one after the other and moved along the same circular path to be collected at a pressure antinode. But there was no coalescence of these minute bubbles, they simply formed a mass of small bubbles. On removing the sound pressure they rose as a body at first but after a few seconds broke away from one another and rose individually to the surface. There appeared to be no interaction between the bubbles as they rose and all bubbles seemed to be moving at the same velocity. From the rising velocity the radius of the bubble was estimated to be 1×10^{-3} cm. It may be worth while noting that the resonant radius of an air bubble at atmospheric pressure is 0.8×10^{-3} cm for a frequency of 428 kc/sec (ref.23).

Five samples of tap water* of different air content were investigated. The thresholds were determined before and after the addition of wetting agent in each case. The results are shown in fig (14).

Two samples of saturated distilled water were also used. The critical pressures measured were - 18.4 and - 20.4 atmospheres. The effect of wetting agent on the

* The tap water used was from a different batch.

threshold of degassed distilled water was not investigated.

5.6 Pressurization

Tap water was used in this experiment. After the tap water had been pressurized in a pressure vessel, it was drawn into the tank and its threshold determined. The maximum pressure applied was 280 lb/in² for a period of 20 minutes. In all the samples tested no noticeable increase in threshold was detected. It was suspected that some water from the reserve tank of the hand pump must have got into the pressurizing vessel and thus contaminated the water inside it. Therefore no description of the pressurizing circuit and results are given.

6. Variation in experimental conditions and repeatability of results

The temperature of water varied between 11°C and 16°C , and no attempt had been made to study the effect of temperature on the cavitation threshold in the present experiment.

The results obtained in the experiments are quite repeatable. As was shown in the experiment that more consistent results were obtained if the same batch of water was used. However when tap water drawn on different days was used, the mean values were quite near to that of the same batch although the scatter between each samples was greater.

Each of the experimental points represents the arithmetical mean of six to eight measurements. The deviation of the individual measurement from the mean is usually less than 5%. But if the water in the focal region was not replaced after a measurement the consequent measurement quite often showed a difference of $\pm 20\%$ from the mean value. It should also be noted that at low air content ($< 50\%$ saturation) a sound pressure 50% higher than the mean value of the threshold for vaporous cavitation could sometime be imposed on the water without any sign of cavitation. It is believed that this is due to the lack of nuclei in the vicinity of the focus. To ensure that the measured threshold represents the characteristics of the whole body of water tested, stirring is necessary in order to bring as many nuclei into the focal region as possible.

The air contents of water samples were determined by using the M.E.R.L. air content apparatus with corrections suggested by Kanellopoulos. The measurements are believed to be within an accuracy of $\pm 1 - 2\%$. The air contents are recorded as c.c./lite water at N.P.T.

7. Discussion

7.1 Effect of free running tap on the threshold of cavitation.

Water drawn quietly from the tap has a higher threshold than that drawn with the tap running free. The effect is believed to be due to the pressurizing of the water in the mains. There is no appreciable difference in the total air content of the water drawn by the two methods and both showed a supersaturation of about 15% at the temperature of the water. Table (1) shows that tap water drawn quietly has a threshold of about 3 atmospheres. This is higher than the threshold of distilled water at the same total air content. The disturbance caused by the free running of the tap decreased the threshold to that of distilled water. Although numerous small bubbles were seen in the body of the tap water drawn in that way, they were not responsible for the decrease in the threshold since the experiments on the ageing of tap water showed that no appreciable increase was noticed for samples which had been standing for 2 - 5 days. Had the bubbles created by the disturbance been responsible for the decrease in threshold, a gradual increase would have been noted as they rose out of the water. This implies that the permanent decrease in the threshold is due to a shift from one equilibrium condition to another as a result of the disturbance.

Some effect of pressurization was still evident for water drawn with free running tap although the effect was partially destroyed by the disturbance on drawing. Fig (7) shows that after the tap water had been standing for 2 - 5 days the first stage of deaeration showed no increase in the threshold for some samples. However on further deaerating the sample a definite increase was noticed. On subjecting the water to a low pressure the remaining effect of pressurization must have been completely destroyed and the nuclei enlarged, but the deaeration caused a reduction in the size of the nuclei. The two effects approximately balanced out and the nucleus size remained almost unchanged although the total air content of the water was lowered.

7.2 Ageing of tap water

Freshly drawn tap water showed no increase in the threshold while it stood in the test tank over a period of 2 - 5 days.

This is at variance with the observations of Blake (ref.9) and Strasberg (ref.12). Both reported that the threshold of freshly drawn tap water increased from about $\frac{1}{2}$ atmosphere to $1\frac{1}{2}$ or $2\frac{1}{2}$ atmospheres over several days. However in the present experiment the threshold of freshly drawn tap water was never less than $1\frac{1}{4}$ atmospheres as shown in table (2). This indicates that the threshold is already too high for the effect to be observed. A possible explanation is that the tap water used in the present experiment has been subjected to a higher pressure than the samples used by Blake and Strasberg or alternatively that their samples were drawn in such a way that the effect of pressurization was completely destroyed.

7.3 Effect of deaeration and re-aeration on the thresholds of cavitation.

The transition from gaseous to vaporous cavitation in tap water took place at a peak sound pressure of $2\frac{1}{2}$ - $2\frac{3}{4}$ atmospheres. This agrees fairly well with the theoretical value calculated by using the formulae derived by Blake (ref.9) i.e., equation (2.1.3) and equation (2.1.4) the peak sound pressure required for causing vaporous and gaseous cavitation at atmospheric pressure are plotted against the sizes of gas nuclei in fig (15). The experimental results for the tap water in fig (9) and fig (10) are plotted to logarithmic scale in fig (16). The agreement in trend is fairly good. It can be observed that the transition from gaseous to vaporous cavitation takes place at a slightly higher sound pressure than that calculated from theory.

If we assume the cavitation thresholds are correctly expressed by equation (2.1.3) and equation (2.1.4) then fig (15) can be used to estimate the sizes of the largest nuclei in the tap water used. At a saturated air content under atmospheric pressure the radius of the nucleus bubble is about 6.6×10^{-5} cm and it decreases to 1.8×10^{-5} cm at 25% saturation.

The variation of the threshold for vaporous cavitation in tap water with total air content is linear as predicted

by the theoretical equations (2.2.3) and (2.3.1) based on the two different concepts of nuclei. In distilled water the same linear variation is observed and on comparison with Strasberg's result on tap water the three lines appear to have the same slope. It may be postulated that the nuclei in tap and distilled tap have the same physical characteristics but the size of the nuclei is smaller in distilled water.

On restoring the air content of tap water no appreciable difference was noticed when the air content was restored either by bubbling air through it or by mixing it with saturated sample. However, when the air content was restored by leaving it standing quietly under atmospheric pressure an increase in the threshold was noted for the same air content. It is believed that when the air content of the sample was restored by standing the original size of the nuclei was not restored. This is the effect of pressurization observed by Strasberg (ref.12), since lowering of the dissolved gas content has the same effect as increasing the hydrostatic pressure. When air was bubbled through the degassed sample the disturbance caused by its passage probably destroyed the effect of undersaturation or alternatively fresh nuclei were introduced into the water, such as dust particles. In the case where saturated water was added the nuclei in the saturated water prevailed and the effect of undersaturation was not observed.

The results of the distilled water were different. No effect of undersaturation was observed. In fact a lowering of the threshold for the same air content was noted. It was thought that this is due to the introduction of new nuclei when the distilled water was transferred to and from the test tank. On bubbling air through degassed distilled water a marked lowering of the threshold was noted. The threshold quickly approached that of tap water for the same air content. This suggested that new nuclei which has the same size as those originally present in the tap water were introduced when air

was bubbled through distilled water.

Effect of filtering on the threshold.

Although only one sample of tap water was filtered and tested, the resulting increase in the threshold was unmistakable. The glass filter used had pores with diameters ranging from 60-100 microns. It is thought unlikely that unattached gas nuclei (10^{-4} to 10^{-5} cm) will be removed in the filtering. It is believed that the physical size of the suspended particles limits the maximum size of the nuclei which can be stabilized on them, and that the nuclei in distilled water were stabilized on suspended particles smaller in size than that of tap water. It is quite possible that these smaller particles were carried over in the distillation process since the distilled water used in the present experiment was made from tap water.

Effect of wetting agent on threshold.

The addition of wetting agent greatly reduced the surface tension of water. It is not known whether the increase in threshold after the addition of wetting agent in saturated tap water was due to the covering up of the hydrophobic crevices or due to the displacement of air from the crevices. For partially degassed tap water the latter seemed to be the case. It is believed that the crevices were completely wetted and the threshold measured (12 atmospheres) was the peak sound pressure required to tear the water away from the wall of the suspended particles in the presence of wetting agent.

The measurement in saturated distilled water showed that the threshold in this case is 19-20 atmospheres.

A summary of the experimental results is given in fig (17).

Strasberg's results on tap water together with the results of Itengar and Richardson are shown in dotted lines.

The results obtained in the present experiment agree in trend with those obtained by Strasberg. It is not known why the results should be so different from that of Iyengar and Richardson.

8. Conclusions

(1) Tap water drawn quietly showed some effect of pressurization but this effect can be partially or completely destroyed by creating a disturbance in the water or subjecting the water to a low pressure.

(2) No ageing of tap water was observed in the present experiment probably due to the size of the nuclei present in the water being too small for the effect to take place.

(3) The transition from gaseous to varorous cavitation was observed and the point of transition measured agrees fairly well with the value calculated theoretically by Blake (ref.9). The linear variation of threshold with air content of water was verified and agreed with the result obtained by Strasberg (ref.12)

(4) Experiments with tap water, distilled water and filtered tap water led to the belief that nuclei in water consist of undissolved air stabilized in the crevices of suspended particles. The physical size of such particles determines the maximum size of the gas nuclei which can be stabilized on them. The removal of the larger suspended particles increased the threshold.

(5) The addition of wetting agent to tap and distilled water greatly increased their resistance to cavitation.

REFERENCES

- (1) Reynolds, O.
"Experiments showing the boiling of water in an open tube at ordinary temperatures" British Assoc. Adv. Sci. Report 1894, p. 564, Science Papers, 2, p.p. 578 - 587.
- (2) Barnaby, S.W.
"On the formation of cavities in water by screw propellers at high speeds" Trans. Inst. Naval Arch. 39, p.p.139 - 144, 1897.
- (3) Parsons, C.A.
"The application of the compound steam turbine to the purpose of marine propulsion" Trans. Inst. Naval Arch. 38, p.p. 232 - 242, 1897.
- (4) Raven, F.A., Feiler, A.M., & Jespersen, Anna
"An Annotated Bibliography of Cavitation" David Taylor Model Basin Report R - 81, 1947.
- (5) Eisenberg, P.
"On the mechanism and prevention of cavitation" David Taylor Model Basin Report 712, 1950.
- (6) Eisenberg, P.
"A brief survey of progress on the mechanics of cavitation" David Taylor Model Basin Report 842A, 1953.
- (7) Eisenberg, P.
"A critical review of recent progress in cavitation research" Cavitation in Hydrodynamics - a Symposium, National Physical Laboratory, U.K. 1955.
- (8) Temperley, H.N.V. & Chambers, LL. G.
"The behavior of water under hydrostatic Tension I" Proc. Phy. Soc. 58, 1946, p. 420.
- (9) Blake, F.G.
"The onset of cavitation in liquids" Acoust. Research Laboratory Harvard University. Technical Memo. No. 12, 1949.

- (10) Connolly, W. & Fox, F.E.
"Ultrasonic cavitation threshold in water" JI. Acoust.
Soc. Am. 26; 843, 1954.
- (11) Galloway, W.J.
"An experimental study of acoustically induced cavitation
in liquids" JI. Acoust. Soc. Am. 26, 849, 1954.
- (12) Strasberg, M.
"The onset of ultrasonic cavitation in tap water" Catholic
University Ph.D. dissertation, 1956.
- (13) Iyengar, K.S., Richardson, E.G.
"The role of cavitation nuclei" Mechanical Engineering
Research Laboratory Fluid Report No. 57, 1957.
- (14) Harvey, E.N., Barnes, D.K., McElroy, W.C., Whitely, A.H.,
Pease, D.C., & Cooper, K.W.
"Bubble formation in animals" JI. Cell. Comp. Physiology,
24, p.p. 23 - 44, 1944.
- (15) Knapp, R.T.,
"Cavitation and nuclei" Trans. A.S.M.E. 80, p. 315,
1958.
- (16) Harvey, E.N., McElroy, W.D., Whiteley, A.H.
"On cavity formation in water" JI. Appl. Phys. 18,
p.p. 162 - 172, 1947.
- (17) McNulty, P.J.
"The M. S. R. L. gas content apparatus" Mechanical
Engineering Research Laboratory Fluid Memo. No. 35, 1955.
- (18) Kanellopoulos, E.V.
"New method for measuring the gas content of water"
Mechanical Engineering Research Laboratory Fluid Report
No. 69, 1950.
- (19) Kanellopoulos, E.V.
"Errors in measuring the gas content of water" Mechanical
Engineering Research Laboratory Fluid Report No. 73, 1958.

(20) Neppiras, E.A. and Naltingk, B.E.

"Cavitation produced by ultrasonics" Proc. Phys. Soc.
London, B, 64, 1032, 1951.

(21) Pode, L.

"Diffusion of air into a pulsating cavitation bubble"
David Taylor Model Basin Report 804, 1955.

(22) Fox, F.E. and Herzfeld, K.F.

"Gas bubbles with organic skin as cavitation nuclei"
Jl. Acoust. Soc. Am. 26, 984, 1954.

(23) Smith, F.D.

"On the destructive mechanical effects of the gas bubbles
liberated by the passage of intense sound through a liquid"
Phil. Mag. 19, 1147, 1935.

LIST OF TABLES

1. Calibration of sound pressure in the focus at different temperature
2. Effect of free running tap on the threshold of cavitation. (tap water)
3. Effect of ageing on the threshold of cavitation. (tap water)

LIST OF FIGURES

1. General view of apparatus.
2. Sketch of test tank.
3. General view of test tank.
4. Block diagram of electronic equipment .
5. Arrangement for bubbling air through water.
6. Calibration curve for sound pressure in the focus of the standing wave against voltage across transducer.
- 6A. Effect of temperature on voltage across transducer and sound pressure in the focus of standing wave.
7. Effect of deaeration on threshold of gaseous cavitation - tap water. (different batch)
8. Effect of deaeration on threshold of vaporous cavitation - tap water. (different batch)
9. Effect of deaeration on threshold of gaseous cavitation - tap water. (same batch)
10. Effect of deaeration on threshold of vaporous cavitation - tap water. (same batch)
11. Effect of re-aeration on threshold of cavitation. (tap water)
12. Effect of re-aeration on the thresholds of cavitation. (distilled water)
13. Effect of deaeration on the thresholds of vaporous cavitation. (distilled water)
14. Effect of wetting agent on the threshold of cavitation. (tap water)

15. Cavitation threshold as a function of bubble radius (theoretical)
16. Cavitation threshold for tap water as a function of air content.
(experimental)
17. Effect of air content on threshold of cavitation. (a summary)

VOLTAGE ACROSS TRANSDUCE IN VOLT	1	2	3	4	5	6	7
	<i>STANDING WAVE</i>						
TEMP. °C	<i>PROBE OUTPUT VOLTAGE IN VOLT x 10³</i>						
9.5	63	112	157	206	246	280	313
10.5	65	110	157	198	245	275	310
11.5	59	108	158	202	237	281	316
12.5	65	110	166	208	249	292	320
13.5	61	117	158	202	240	276	312
14.5	65	112	157	200	246	280	320
15.5	62	108	157	202	243	275	312
MEAN VALUE	63	111	158	203	244	280	315
MAXIMUM DEVIATION	±6%	±5%	±5%	±2%	±3%	±4%	±2%
PEAK SOUND PRESSURE IN ATM.	0.54	0.94	1.33	1.73	2.10	2.38	2.78
	<i>PROGRESSIVE WAVE</i>						
	<i>PROBE OUTPUT VOLTAGE IN VOLT x 10³</i>						
	76	142	188	225	277	310	350
PEAK SOUND PRESSURE IN ATM	0.65	1.21	1.59	1.92	2.36	2.64	2.98

**TABLE - 1 CALIBRATION OF SOUND PRESSURE
IN THE FOCUS AT DIFFERENT
TEMPERATURES**

EXPT. NO.	1	2	3	4	5	6
<i>PEAK SOUND PRESSURE IN ATMS.</i>						
<i>FREE RUNNING TAP</i>	2.12	2.12	2.32	2.12	2.08	1.60
<i>DRAWN QUIETLY</i>	2.44	2.68	2.96	3.16	3.16	2.44
<i>TEMP. °C</i>	14	13	13	14	14	11

TABLE-2 EFFECT OF FREE RUNNING TAP ON THRESHOLD OF CAVITATION (TAP WATER)

EXPT. NO.	1	2	3	4	5	6
<i>TIME AFTER FILLING PEAK SOUND PRESSURE IN ATMS.</i>						
<i>1 HOUR</i>	1.56	1.50	1.74	1.56	1.70	1.72
<i>2 "</i>	1.72	1.62	2.16	1.56	1.98	1.54
<i>4 "</i>	1.76	1.40	2.12	1.62	2.02	1.46
<i>6 "</i>	1.70		2.16	1.60	1.72	
<i>8 "</i>	1.56	1.56		1.50	1.76	
<i>18 "</i>			2.06			1.64
<i>24 "</i>	1.72	1.26	2.06	1.34		1.46
<i>30 "</i>	1.76	1.42				1.80
<i>48 "</i>	1.95	1.46	2.16		2.06	1.56
<i>68 "</i>		1.46			2.10	1.76
<i>78 "</i>		1.42				1.72
<i>120 "</i>						1.72

TABLE-3 EFFECT OF AGEING ON THRESHOLD OF CAVITATION (TAP WATER)

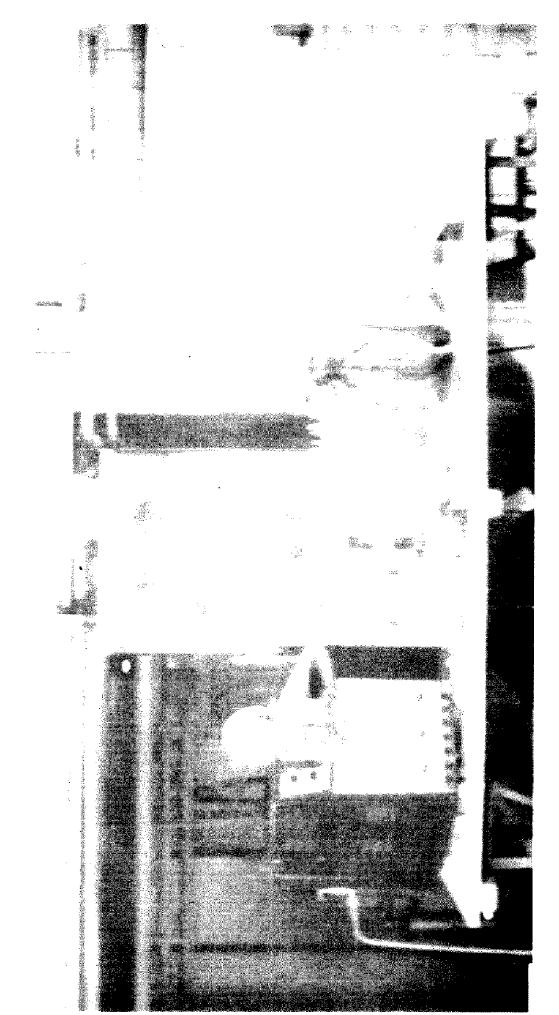


FIG. 1 General View of apparatus

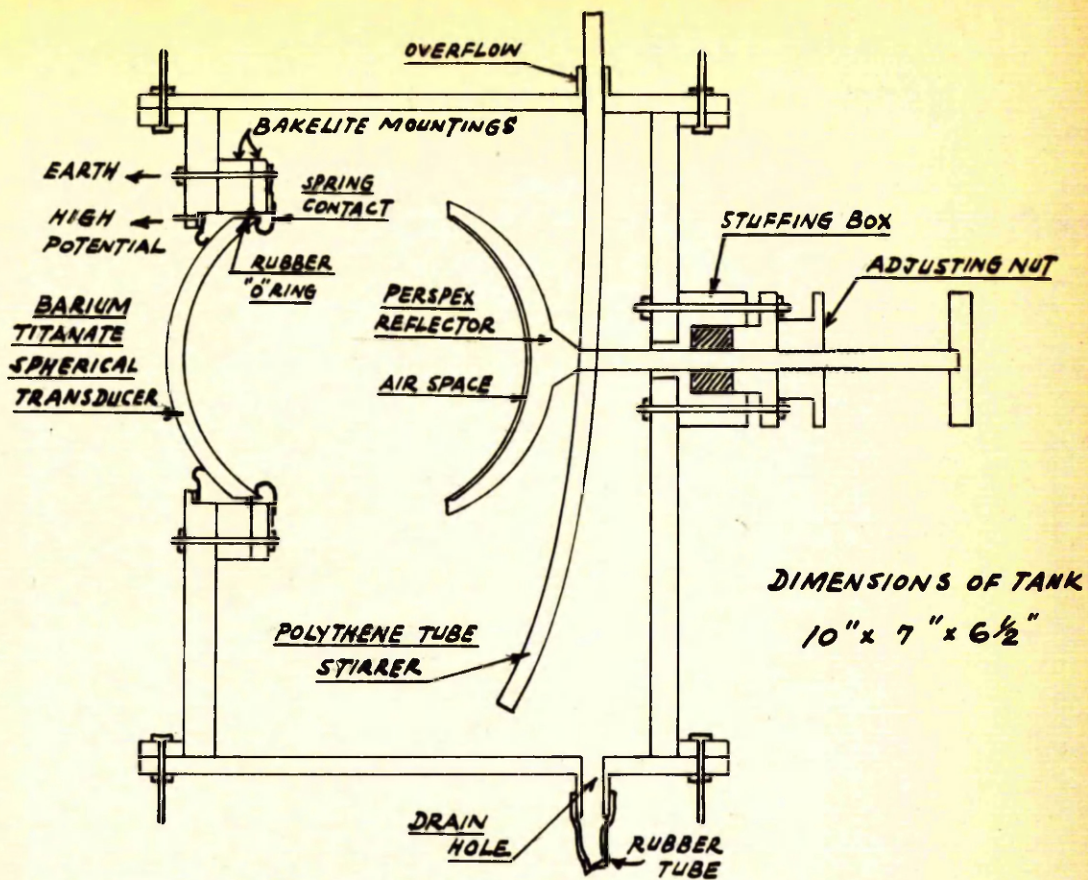


FIG-2 SKETCH OF TEST TANK

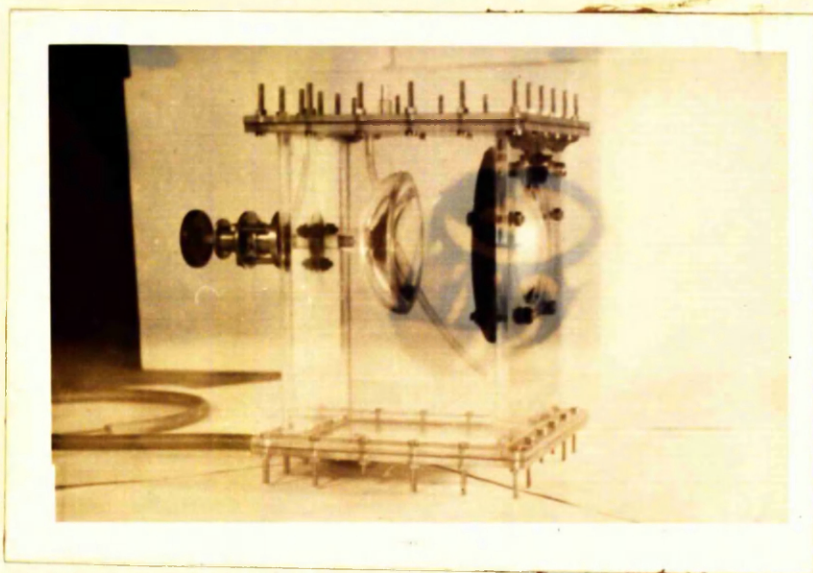


FIG-3 GENERAL VIEW OF TEST TANK

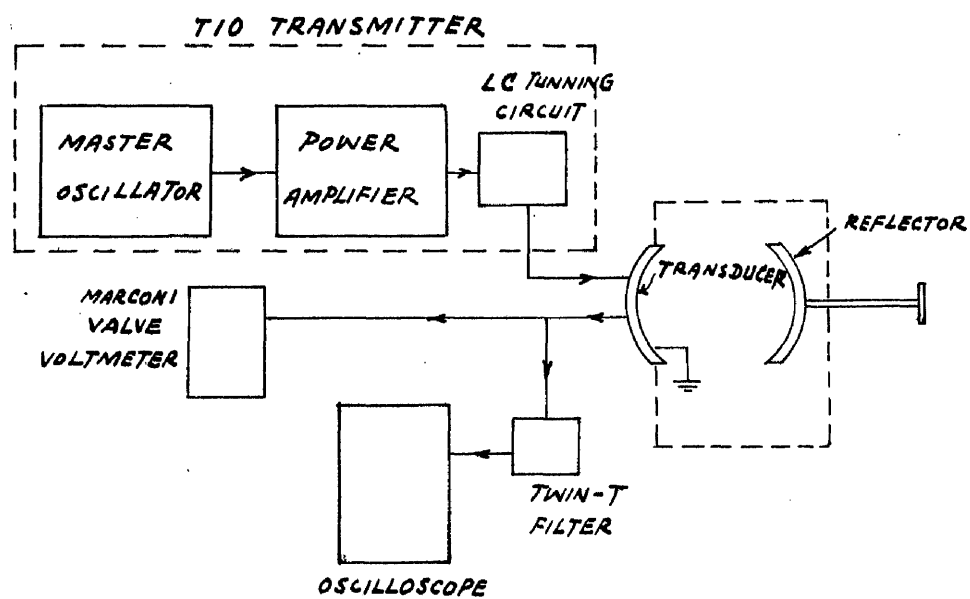


FIG - 4 BLOCK DIAGRAM FOR ELECTRONIC EQUIPMENT

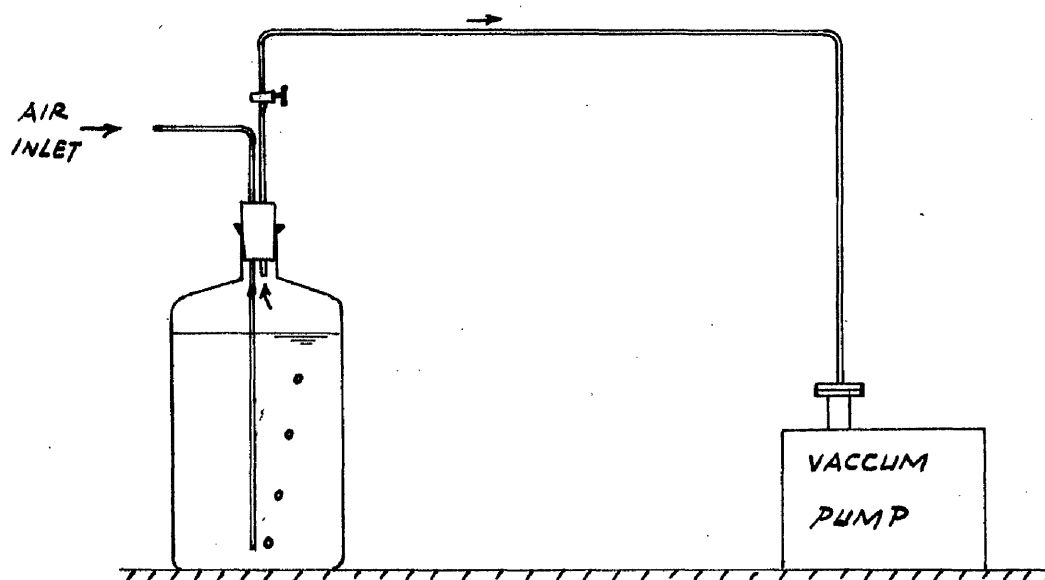


FIG-5 ARRANGEMENT FOR BUBBLING AIR THROUGH WATER

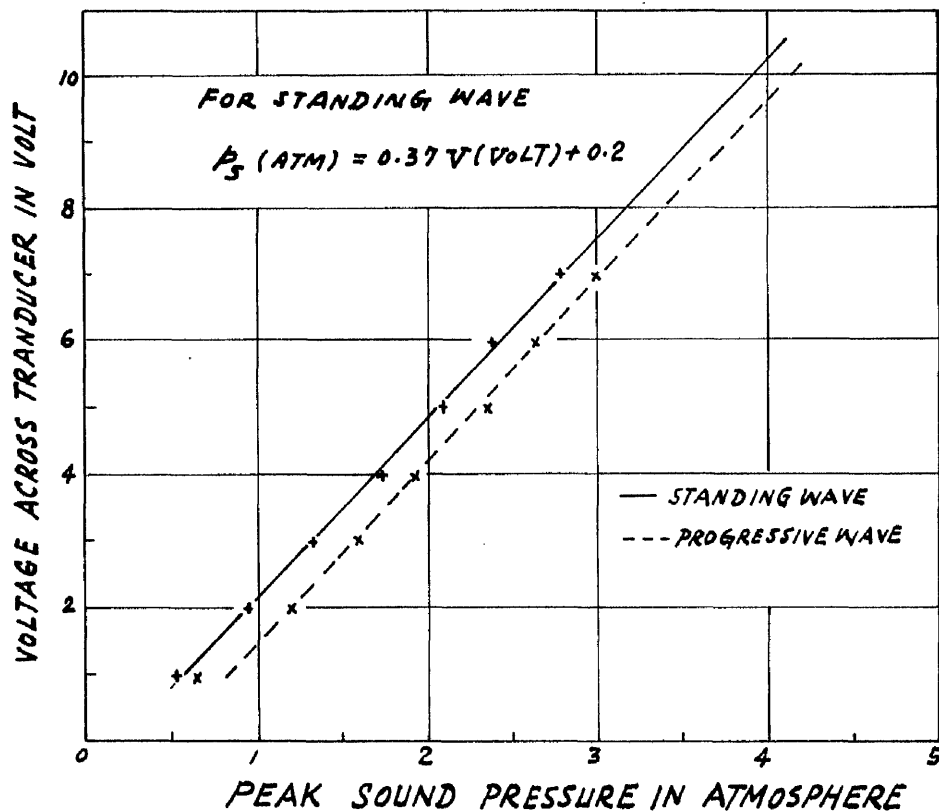


FIG-6 CALIBRATION CURVE FOR SOUND PRESSURE IN THE FOCUS OF THE STANDING WAVE AGAINST VOLTAGE ACROSS TRANSDUCER

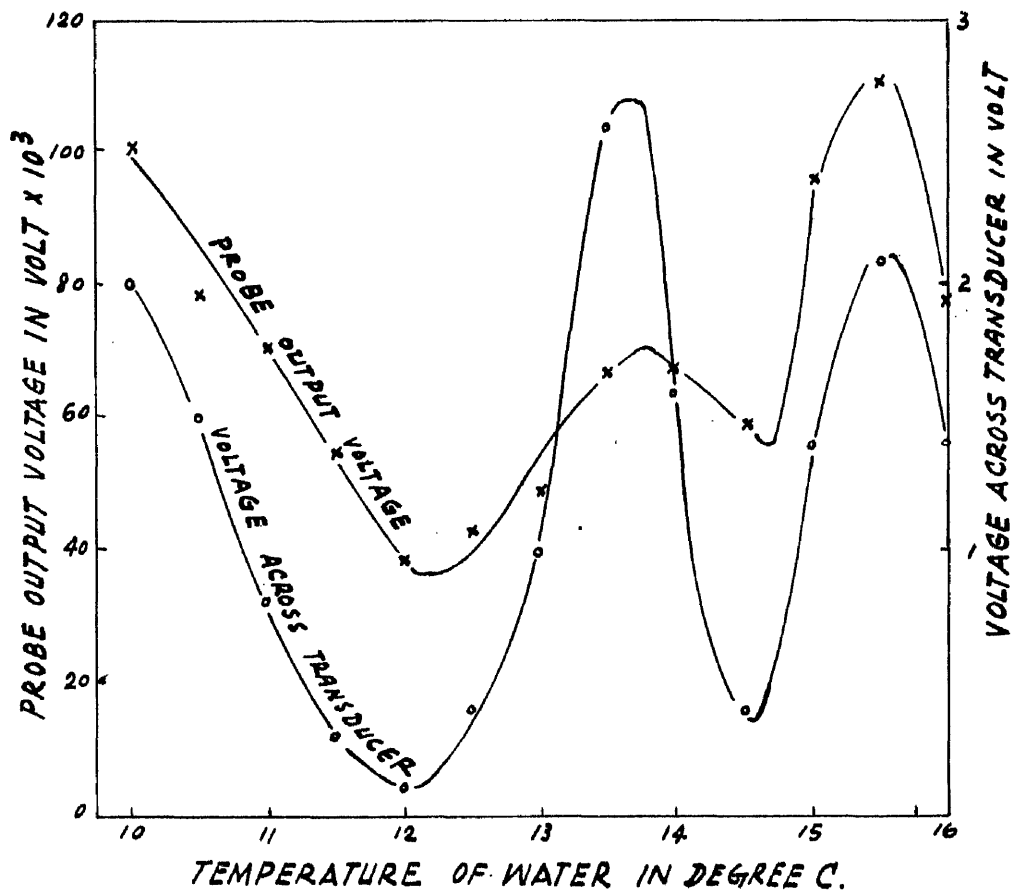


FIG-6A EFFECT OF TEMPERATURE ON VOLTAGE ACROSS TRANSDUCER AND SOUND PRESSURE IN THE FOCUS OF STANDING WAVE

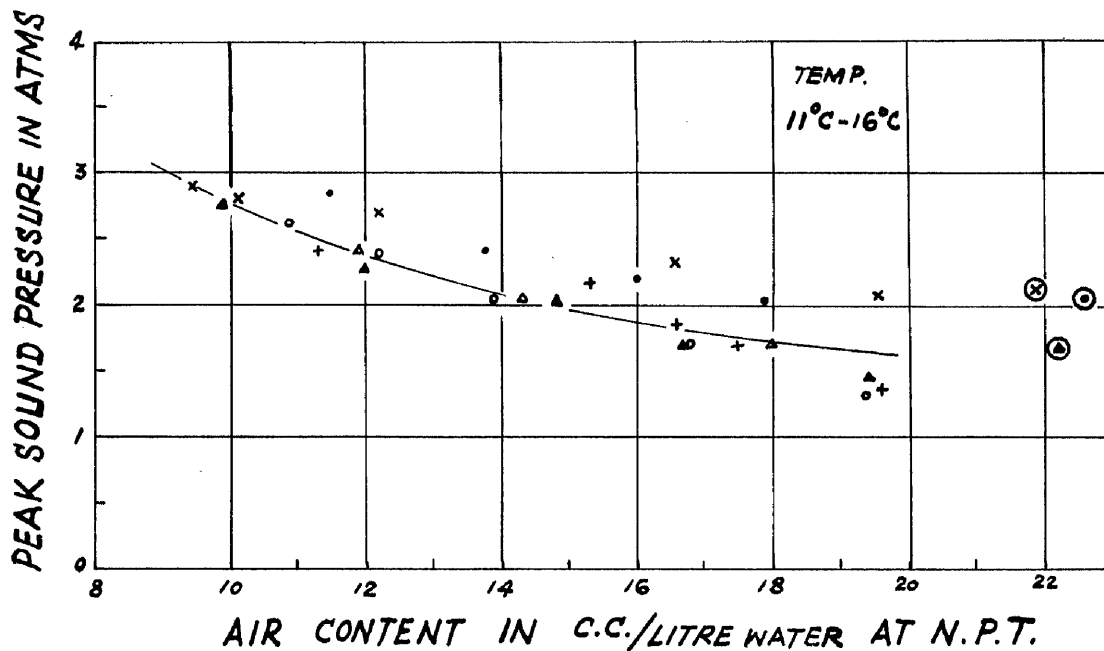


FIG - 7 EFFECT OF DEAERATION ON THRESHOLD OF GASEOUS CAVITATION (TAP WATER) - DIFFERENT BATCHES

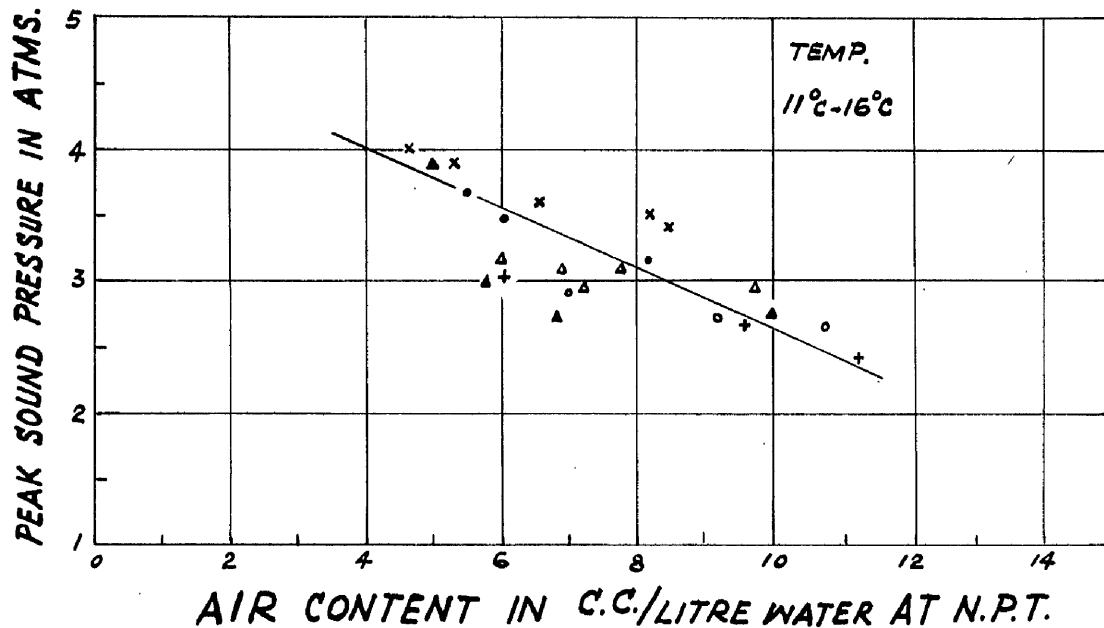


FIG - 8 EFFECT OF DEAERATION ON THRESHOLD OF VAPOROUS CAVITATION (TAP WATER) - DIFFERENT BATCHES

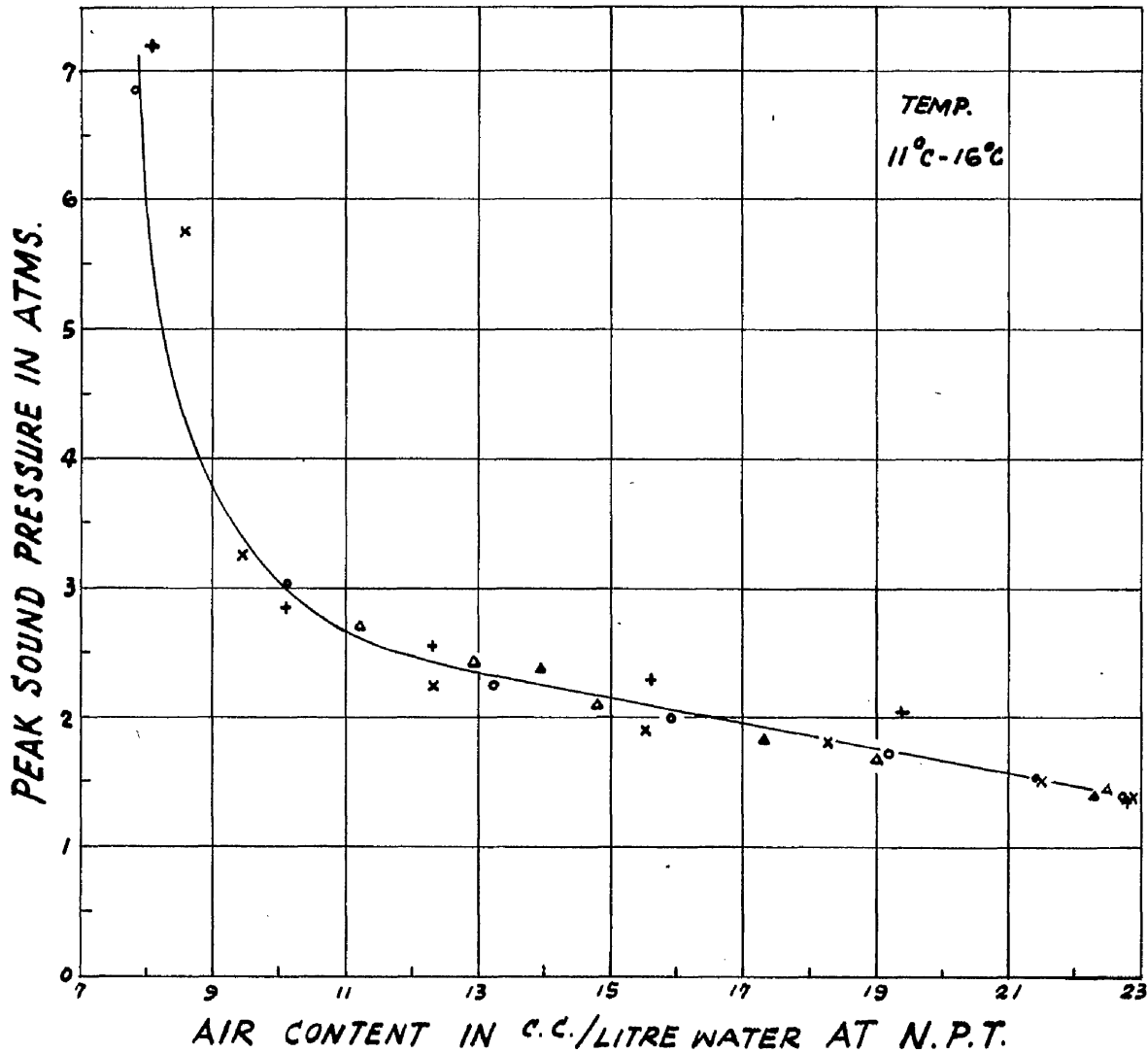


FIG-9 EFFECT OF DEAERATION ON THE THRESHOLD OF GASEOUS CAVITATION (TAP WATER) - SAME BATCH

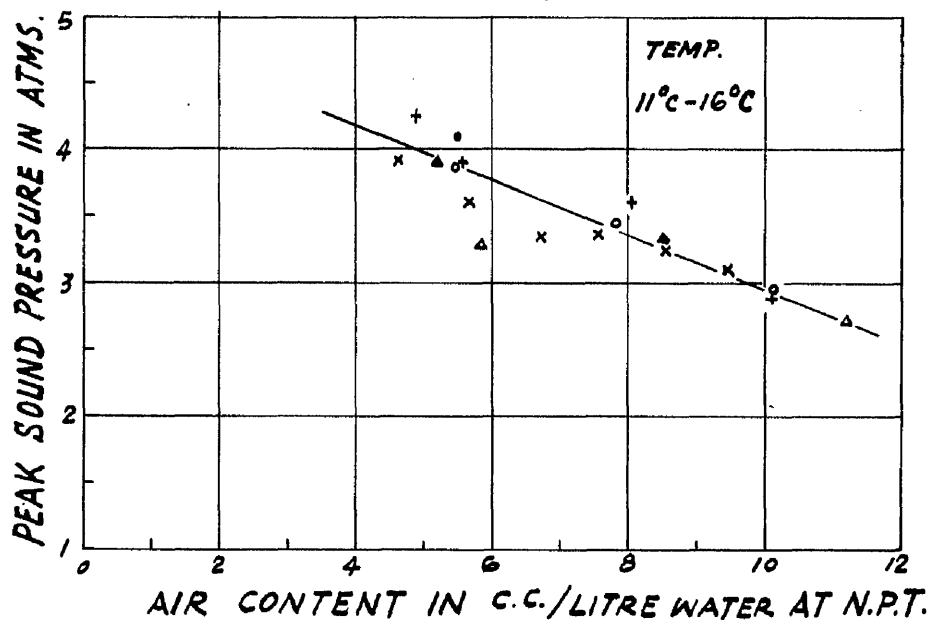


FIG-10 EFFECT OF DEAERATION ON THE THRESHOLD OF VAPOROUS CAVITATION (TAP WATER) - SAME BATCH

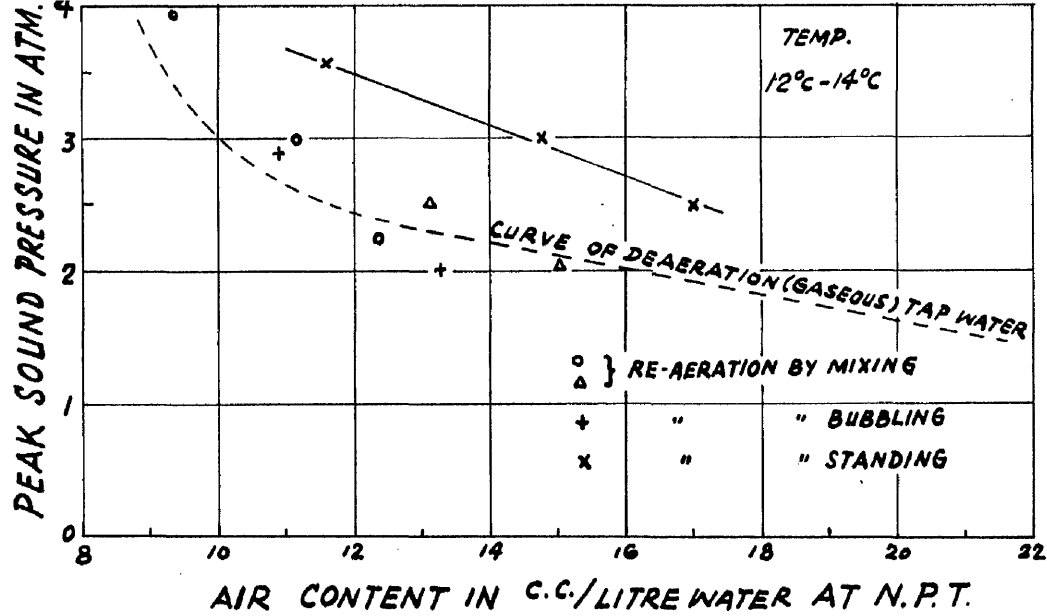


FIG-11 EFFECT OF RE-AERATION ON THRESHOLD OF CAVITATION (TAP WATER)

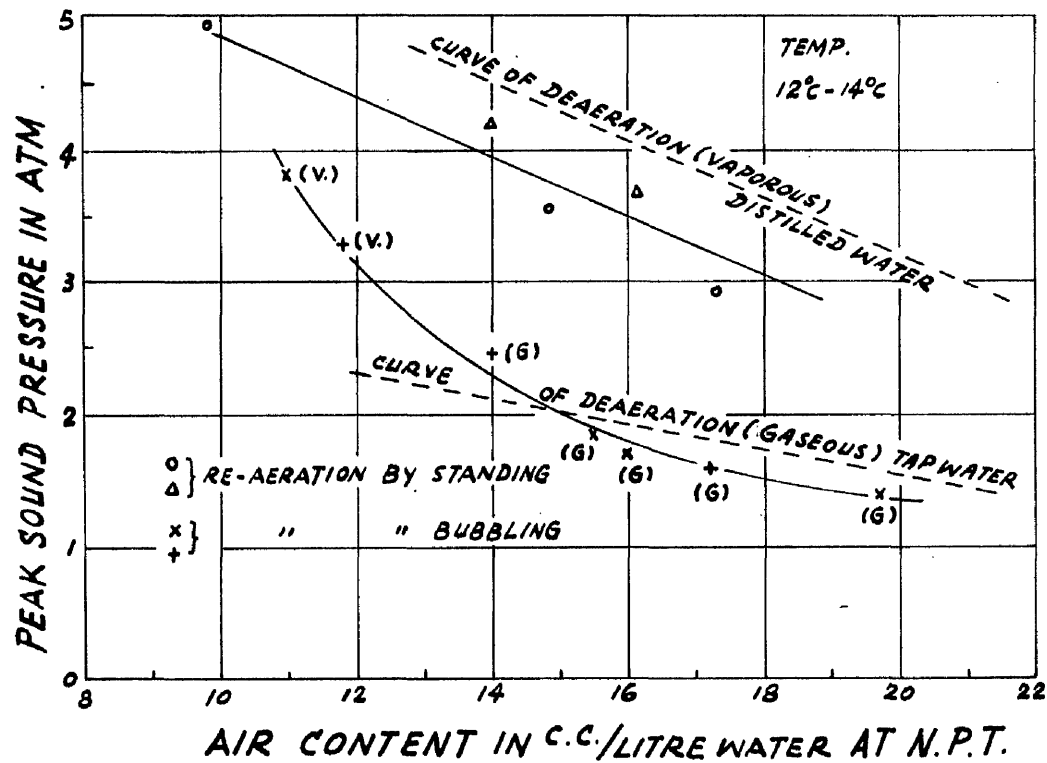
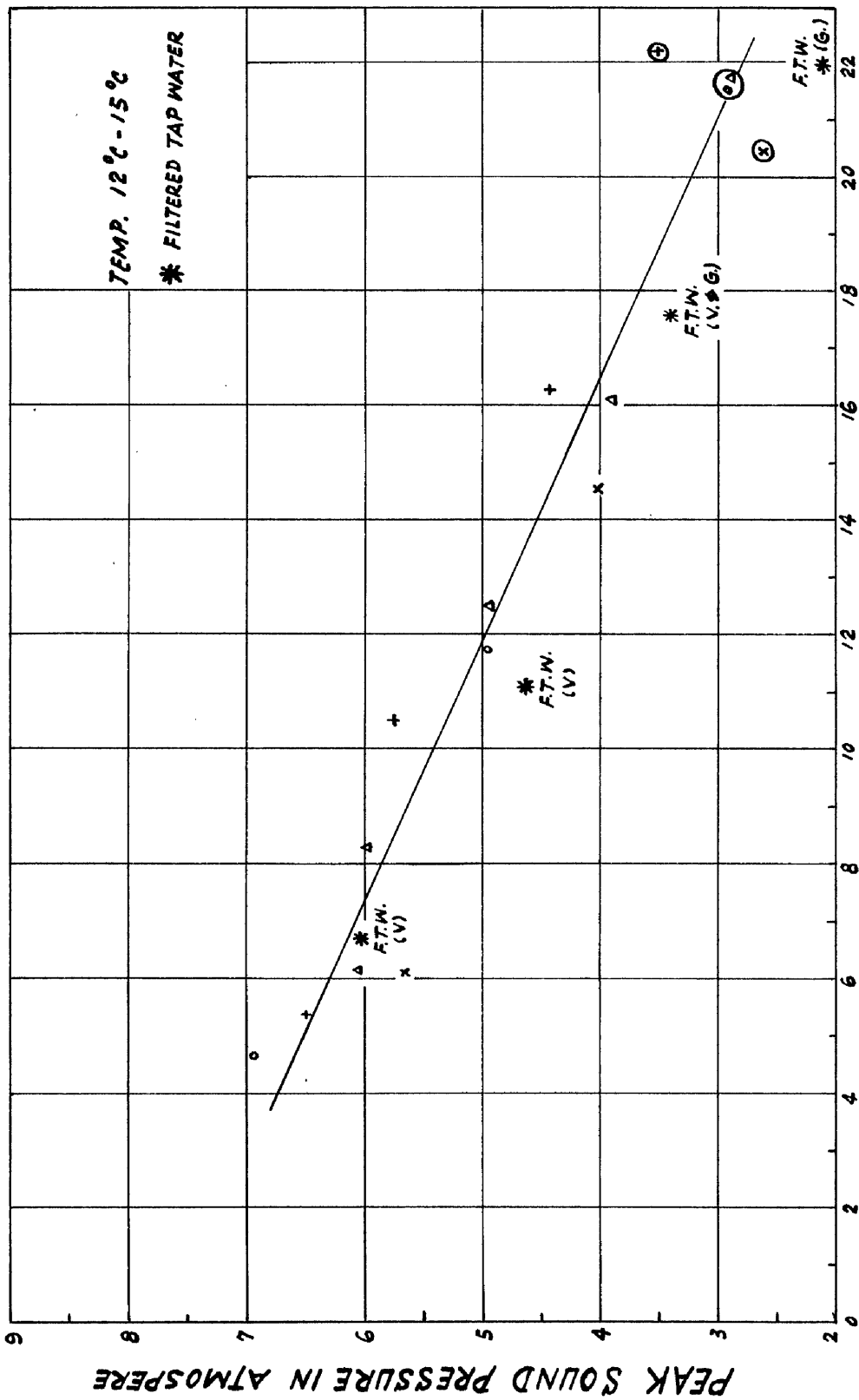
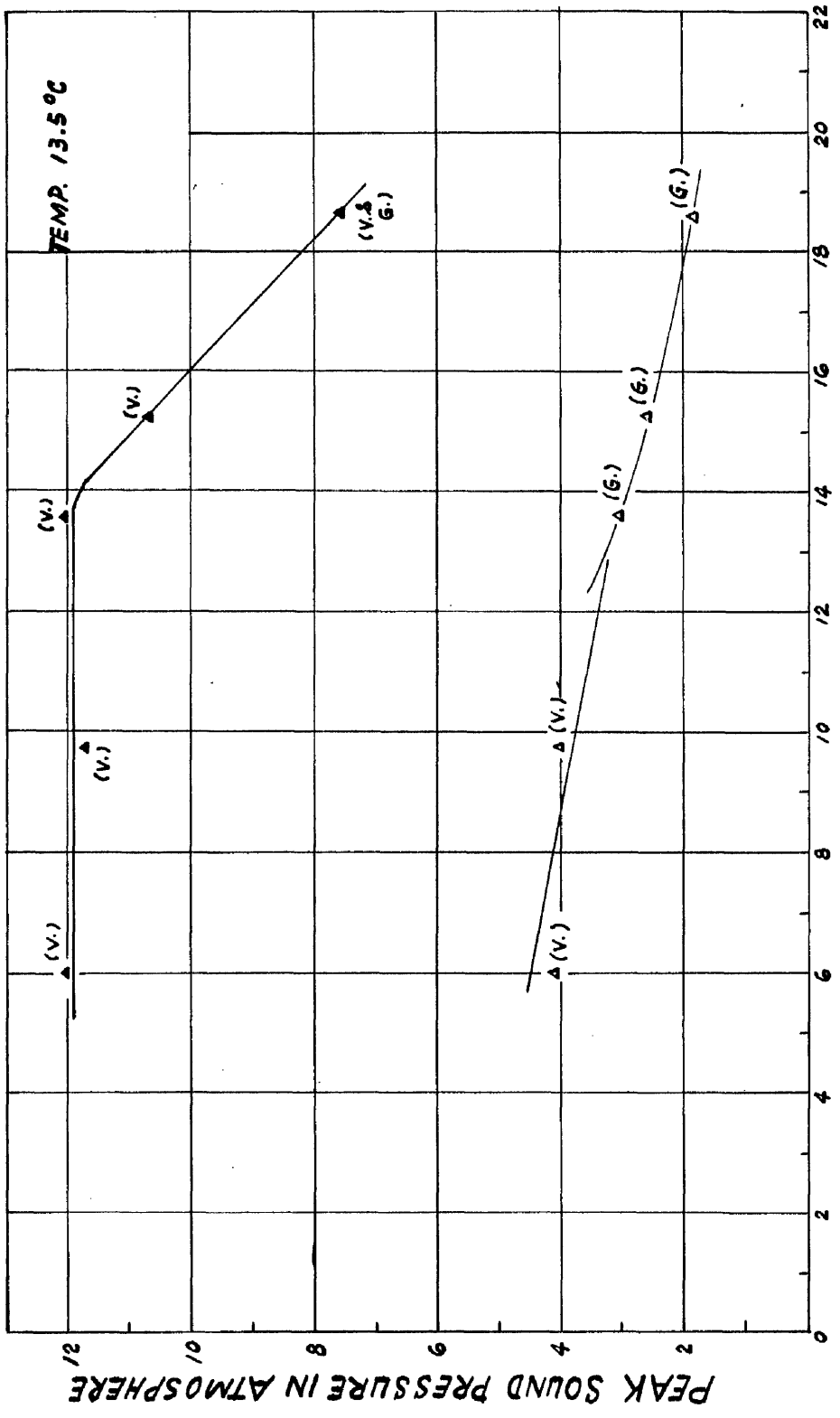


FIG-12 EFFECT OF RE-AERATION ON THE THRESHOLD OF CAVITATION (DISTILLED WATER)



AIR CONTENT IN C.C./LITRE WATER AT N.P.T.
 FIG-13 EFFECT OF DEAERATION ON THE THRESHOLD OF VAPOROUS
 CAVITATION (DISTILLED WATER)



AIR CONTENT IN C.C./LITRE WATER AT N.P.T.
 FIG-14 EFFECT OF WETTING AGENT ON THRESHOLD
 OF CAVITATION (TAP WATER)

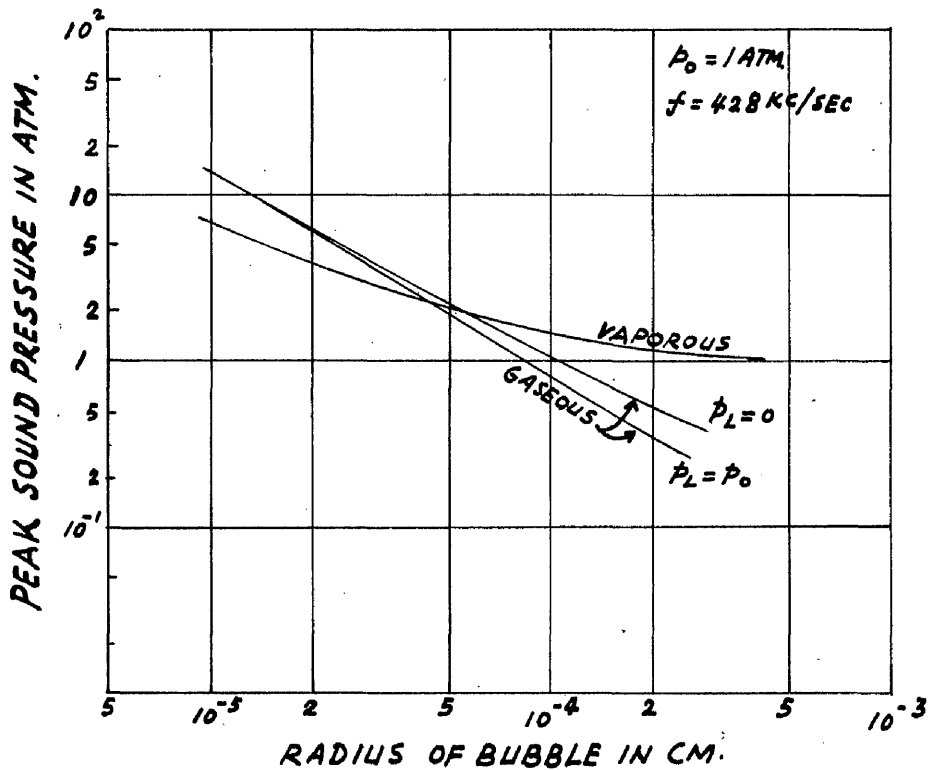


FIG-15 CAVITATION THRESHOLD AS A
 FUNCTION OF BUBBLE RADIUS
 (THEORECTICAL)

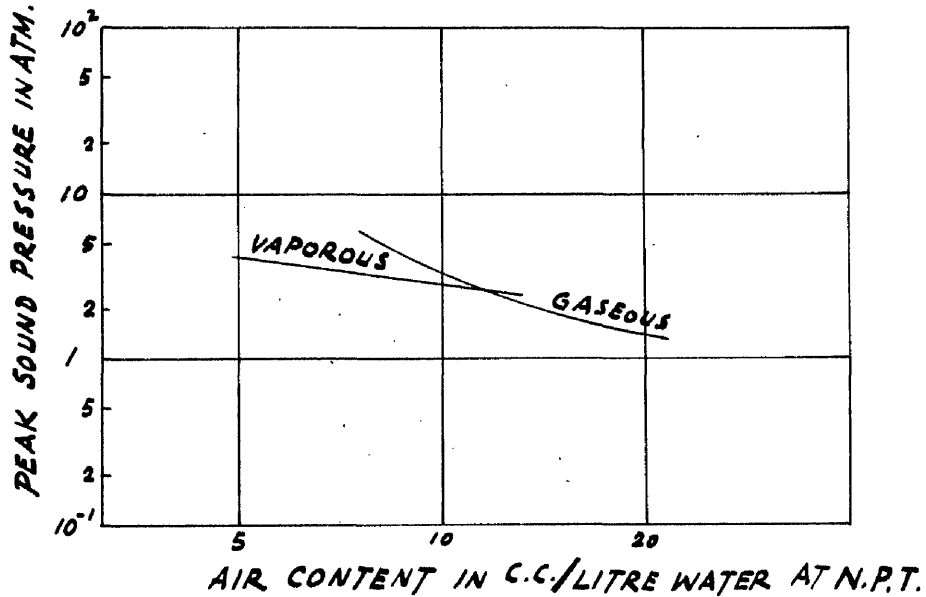
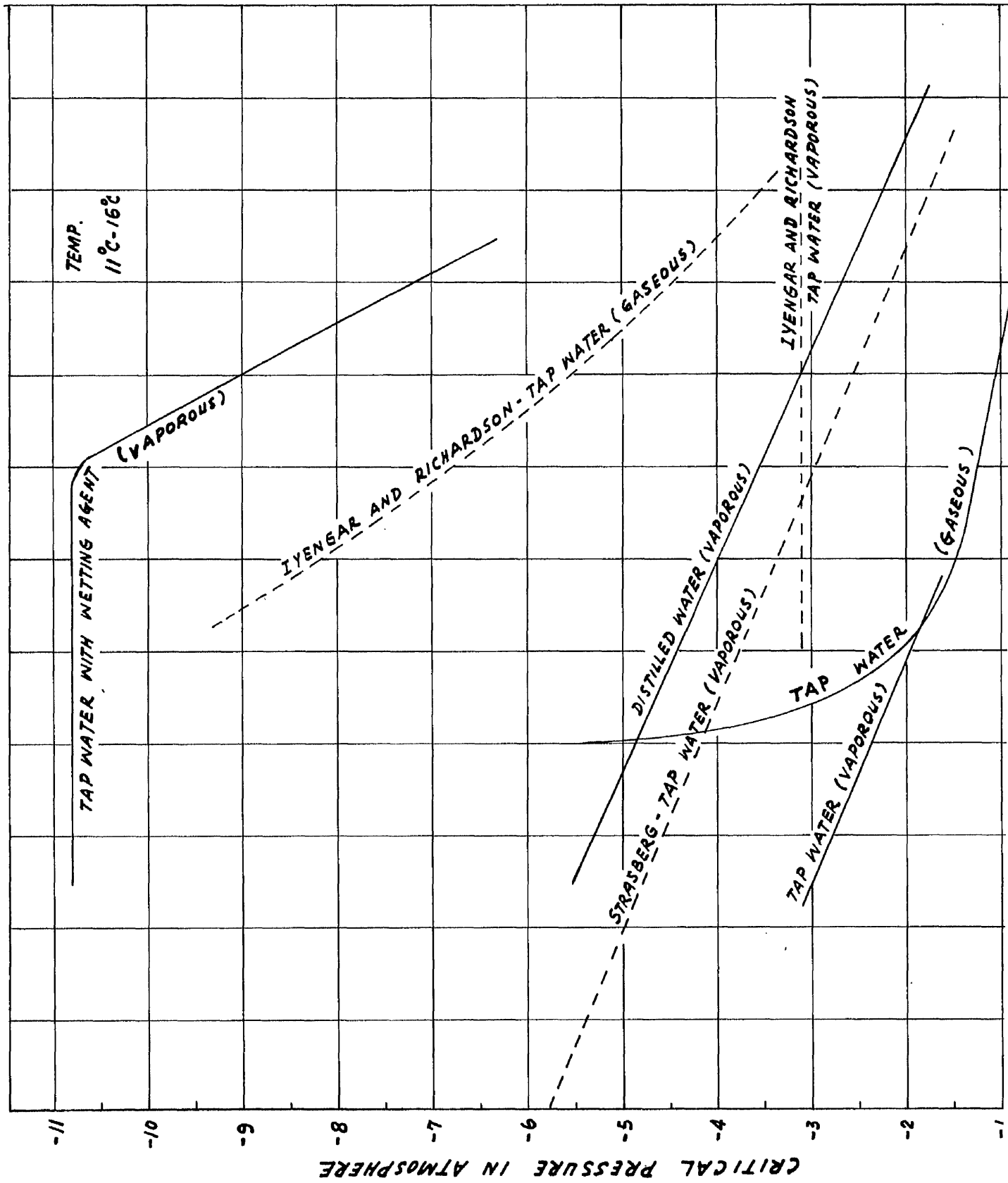


FIG-16 CAVITATION THRESHOLD FOR TAP
 WATER AS A FUNCTION OF AIR
 CONTENT (EXPERIMENTAL)



(PART II)

RESORPTION OF AIR BUBBLES

LIST OF SYMBOLS USED

- K_L --- liquid coefficient (ft/sec)
- $X_1 X_2 X_3$ --- height above datum line (ft)
- v --- rising velocity of small air bubble (ft/sec)
- $\frac{dv}{dt}$ --- rate of decrease of rising velocity of small air bubble
(lb/sec²)
- t --- time (sec)
- p_{X_3} --- ambient pressure (abs.) of water in main tube at a height
 X_3 above datum line (lb/ft²)
- p_b --- atmospheric pressure (lb/ft²)
- w_m --- density of mercury (lb/ft³)
- w_w --- density of water (lb/ft³)
- p_g --- pressure of air inside bubble (lb/ft²)
- σ --- surface tension (lb/ft)
- r --- radius of bubble (ft)
- p_v --- vapour pressure of water (lb/ft²)
- p_L --- saturation gas pressure for a gas concentration of C_L
in water (lb/ft²)
- S --- $\frac{p_L}{p_g}$
- w --- weight of gas in bubble (lb)
- A --- interface area (ft²)
- C_g --- concentration of gas in water saturated at a gas pressure
 p_g (lb/ft³)
- C_L --- concentration of gas in water saturated at a gas pressure
 p_L (lb/ft³)
- $\frac{dw}{dt}$ --- rate of transfer of gas (lb/sec)
- R --- gas constant (ft/°K)
- T --- temperature of water (°K)
- H --- Henry's constant (ft⁻¹)
- g --- acceleration due to gravity (ft/sec²)
- ρ --- mass density of water (lb sec²/ft⁴)
- ρ' --- mass density of air in bubble (lb sec²/ft⁴)
- μ --- viscosity of water (lb sec/ft²)

K_{L_2} --- K_L for region outside Stoke's (ft/sec)

K_{L_1} --- K_L for Stoke's region (ft/sec)

V --- velocity of flow (ft/sec)

p --- ambient pressure (lb/ft²)

p_0 --- ambient pressure at time $t = 0$ (lb/ft²)

r_0 --- radius of bubble at time $t = 0$ (ft)

VALUES OF CONSTANTS USED

$$\sigma = 5.44 \times 10^{-6} \text{ lb/ft}$$

$$p_v = 33 \text{ lb/ft}^2$$

$$R = 96 \text{ ft/}^\circ\text{K}$$

$$T = 286.5 \text{ }^\circ\text{K}$$

$$H = 8.59 \times 10^{-7} \text{ ft}^{-1}$$

$$g = 32.2 \text{ ft/sec}^2$$

$$\rho = 1.939 \text{ lb sec}^2/\text{ft}^4$$

$$\mu = 24.85 \times 10^{-6} \text{ lb sec/ft}^2$$

1. Introduction.

Much interest has been shown in recent years in the absorption of air bubbles in undersaturated water. This is intimately connected with the study of cavitation on models in water tunnels. When cavitation occurs on a model in the working section of a water tunnel with the air content of the tunnel water near saturation a large number of small bubbles containing a mixture of air and water vapour are formed on the collapse of the cavitation bubbles. These bubbles are entrained and recirculated unless means are provided for their removal or re-absorption (resorption). Their presence in the tunnel water prevents the satisfactory operation of the tunnel for long periods and may affect the results of experiments on cavitation inception where the size of the cavitation nuclei is an important factor in determining the inception pressure. The physical removal of these free bubbles will alter the total dissolved air content of the tunnel water and may affect the experimental results. Therefore to maintain a constant dissolved air content of the tunnel water as well as a bubble-free operational condition in the working section it is necessary to force these free air bubbles formed by cavitation back into solution before the water returns to the working section.

The first practical device for achieving the aim outlined above was constructed at the Hydrodynamic Laboratory of the California Institute of Technology and was termed a "Resorber" (See ref.1). It is essentially a deep cylindrical pit which forms a part of the tunnel circuit. Water from the working section is led into the "resorber" and with vertical tubes and partitions is allowed to spend enough time under pressure to re-dissolve any free air bubbles entrained in the water. Many resorbers have been constructed since (see ref 2, 3 and 4). The design of the resorber and the determination of its physical dimensions depend on information obtained from the analysis of the rate of re-absorption (resorption is to be used in the following text) of air bubbles in undersaturated water under conditions similar to those encountered in the water tunnel. The first of such analysis is by Brown (ref,5) who worked out a resorption equation for air bubbles under a constant external pressure equal to the mean pressure in the resorber.

A more recent analysis which takes into account the continuously varying external pressure as the bubble is transported up or down the vertical limbs of the resorber is provided by Silverleaf (ref.4). The basis of both analyses is the Lewis-Whitman concept of liquid and gas film (ref 6) in dealing with the transfer of air through the bubble wall. The Lewis-Whitman equation for a gas of low solubility therefore forms one of the basic equations in their analyses (for Lewis-Whitman equation see section (5.1) eqn.(5.1.1)). The empirical liquid coefficient K_L is thus of direct importance in determining the time required for resorbing an air bubble of a certain size under a constant or varying external pressure.

Little information is available on the numerical value of K_L which can be applied to evaluate the rate of resorption of small air bubbles under water tunnel conditions. Brown (ref 5) found from experiment in the original water tunnel (without resorber) that the resorption equation with $K_L = 6.3 \times 10^{-4}$ ft/sec fitted the upper limit of the experimental data. Since the velocity of flow in the resorber will be much less than the velocities used in the experiment with a correspondingly lower level of turbulence, Brown thought that the actual value of K_L should be between 3.3×10^{-4} ft/sec (36 cm/hr) and 6.3×10^{-4} ft/sec (70 cm/hr). Silverleaf (ref 4) used a value of K_L equal to 4.5×10^{-4} ft/sec in his calculation although a value of 2.7×10^{-4} ft/sec was also used. The only other experiment which was designed to measure the rate of resorption of air bubbles under conditions similar to those encountered in water tunnels is that of Silberman (ref 7). Resorption of air bubbles took place inside a perspex cylinder. The air bubble under study was kept from rising by rotating the water inside the cylinder with a rotor plate which also served as a turbulence generator. For the most turbulent case in his experiment and with the air content of water equal to zero Silberman obtained a value for K_L equal to 6.4×10^{-4} ft/sec. His experiment was carried out at a temperature of 39°C these values of K_L form the upper limit of conditions encountered in water tunnels. For the satisfactory design of the resorber it is rather the lower limit of the value of K_L which is more important.

The present experiment was designed to evaluate K_L for conditions corresponding to the lower limit encountered in water tunnels.

1.1 Aim of the experiment

The aim of the present experiment was to study the resorption of air bubble under laminar flow conditions. Since K_L increases with increasing amount of agitation (or turbulence) (ref 8) the study under such conditions will provide the lower limit required. This was achieved by studying the resorption of small air bubbles rising in under saturated water. The effects of other factors such as air content of water, external pressure and bubble size on K_L were also studied. No attempt was made to evaluate the effect of temperature on K_L in the present experiment though there is evidence that K_L increases with increasing temperature (ref 9).

2. Design and Description of Apparatus.

In designing an experiment to achieve the aim outlined in the last section a few requirements have to be met by the apparatus.

- (1) The apparatus must be long enough for a noticeable change in the size of the bubble to be observed.
- (2) Some means of increasing the ambient pressure of the water must be provided.
- (3) A method must be found to introduce different sizes of small air bubbles into the apparatus under ambient pressures that may be higher than that of atmospheric.

The air bubbles must be produced by a cavitation process so they will have the same composition as the bubbles produced by cavitation in water tunnel, namely $\frac{2}{3}$ nitrogen and $\frac{1}{3}$ oxygen.

- (4) The rate of resorption of the small air bubbles must be measured accurately and continuously so that a complete record may be obtained to show the effect of air content of water, ambient pressure and bubble sizes.

2.1 The Main tube.

A sketch of the apparatus is shown in Fig.(1), it consists of a 7 foot long glass tube of one inch inside diameter. The top of the tube is terminated by a two way glass cock J_1 which is connected to another three-way glass cock J_2 by means of polythene tubing. By turning J_2 one can either connect the main tube to drain or open it to atmosphere. The purpose of having J_2 is explained in section (3.2). A three-way glass cock J_3 forms the bottom end of the tube. J_3 provides the tube with a connection either to inlet or the mercury reservoir Q_1 .

2.2 Pressurization

The increase in the ambient pressure of water is achieved by elevating the mercury reservoir Q_1 which moves along a vertical track mounted on a board upon which the main tube is also fixed. With a string and an overhead pulley Q_1 can be moved to any desired position corresponding to the ambient pressure required and will remain there with the help of a jamming cleat. The actual ambient pressure of water in the tube is measured by means of a mercury manometer directly connected to the tube.

2.3 Bubble generation

The bubble generator consists of a length of capillary tubing of $\frac{1}{32}$ m.m. bore, two-glass cocks J_4 and J_5 and a small mercury reservoir Q_2 . The open end of the capillary tubing is made into a nozzle and sealed into the main tube. The generation of bubbles is described in section (3.3).

2.4 Measurement of rate of resorption

In order to measure the rate of solution of small air bubbles under different experimental conditions it is important to know the size of the bubble at any instant under one set of experimental conditions. Direct measurement of the size of an air bubble rising in the main tube would involve photographing such a small moving object at different points along the tube. To obtain an image sharp enough for

measurement at various points will be difficult since not all the bubbles generated will rise in exactly the same vertical line.

It was decided to measure the rising velocity of such small bubbles at various points along the main tube instead. The rate of decrease of the bubble radius can then be calculated from the decrease in rising velocity measured. This required the plotting of a time-distance curve for each individual bubble. The slope of the curve at any instant gave the instantaneous rising velocity of the bubble.

Perspex marker rings with a hair-line at the centre of each are placed at fixed distances along the tube and the times at which the bubble passed the hair-lines of certain markers were recorded by means of a 8 m.m. cine-camera with a 38 m.m. lens operated by remote control to photograph the dial of a stop-watch single shot. By this system as many readings as required can be obtained without any difficulty for one bubble and the whole experiment is within the capability of one person. The arrangement is shown in Fig (2).

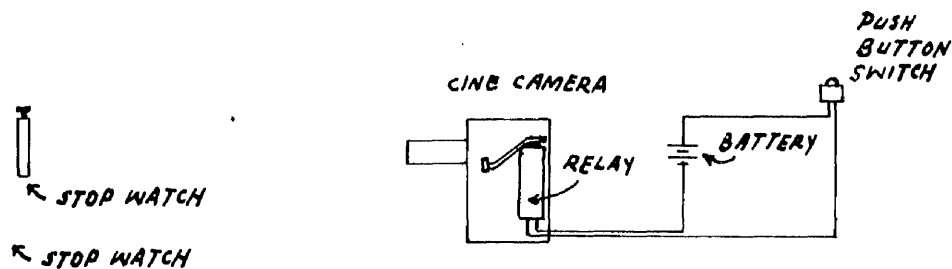


FIG - 2 ARRANGEMENT FOR CINE CAMERA

2.5 Lighting

Lighting of the main tube is provided by a long fluorescent tube which illuminates the whole length of the tube through a slot in the board with equal intensity and does not cause any appreciable heating of the water in the main tube over long periods. The board was painted black and the bubbles were viewed against this dark background.

2.6 Air content of water.

The air content of the water was determined

by using the M.E.R.L. air content apparatus (ref 10) with corrections suggested by Konellopoulos (ref 11 and 12).

3. Experimental Procedure and Technique.

To measure the instantaneous rising velocity of small air bubbles under various experimental conditions in the present apparatus the typical procedure followed for one experiment is described in the following.

3.1 Preparation of Water

Tap water was used in all the experiments since this is the water used in most water tunnel experiments. To achieve a desired air content tap water in a large glass bottle was evacuated by means of a vacuum pump. The bottle was rocked continuously to accelerate the removal of air from the water. When a rough reckoning indicated that the desired air content had been reached the evacuation was discontinued and the water transferred to the long glass tube. With J_1 open, J_2 turned to drain and J_3 to inlet (see Fig 1.) and with the glass bottle held high above the main tube, the long rubber tube connected to the inlet was inserted into the glass bottle. A light suction applied to the rubber tube which leads from J_2 to drain started water siphoning into the main tube from the glass bottle. The water was allowed to run to waste until about two complete changes of water had been effected in the tube. J_1 was then closed and J_3 turned to the position for connecting the main tube with the mercury reservoir Q_1 . A sample was withdrawn immediately from the water remaining in the bottle to determine the actual air content of water used.

3.2 Setting ambient pressure.

J_2 was then turned to atmosphere and J_1 opened to let the whole system return to atmospheric pressure. (the open end of the rubber drain tube was at a lower position than the main tube, the ambient pressure inside the tube was slightly

under atmospheric when J_1 was first closed.) With J_4 opened and J_5 closed J_1 was again closed and the mercury reservoir elevated to the desired position. When the mercury levels in the manometer and in the small mercury reservoir Q_2 became steady the apparatus was ready to receive its first bubble.

3.3 Bubble Generation

The stop-watch was then started. To generate bubbles of different sizes J_4 was closed and Q_2 lowered to reduce the pressure in the capillary tubes behind J_4 (all the tubes are filled with water). Air started to come out of solution and was collected at the inlet to J_4 to form a small air bubble. On opening J_4 and by manoeuvring Q_2 the small air bubble was transported to the horizontal portion of the capillary tubing. Here, by the action of throttling with Q_2 the small air bubble was broken into a number of smaller bubbles. This required a certain amount of practice but once the necessary technique was mastered minute air bubbles could be produced at will. By means of Q_2 the desired minute bubble was transported to the base of the nozzle where it rose into the main tube under its own buoyancy. Care was taken not to impart any initial velocity to the bubble by forcing it out of the nozzle. When that happens the bubble was ignored. When the bubble left the nozzle J_4 was closed and Q_2 replaced on its holder. Bubbles of different sizes could be generated by this method even under ambient pressure much higher than atmospheric since the pressure difference was taken up by the mercury levels in the polythene tube connecting the reservoir Q_2 and the capillary tubing and had no effect on the working of this part of the apparatus.

3.4 Time-Distance Record

A distance of 9" separated the nozzle and the first marker ring to allow the bubble enough time to attain

its terminal velocity. When the bubble passed the hair-line of the first marker ring, the button was pressed and the time shown on the stop-watch was recorded on the film of the 8 m.m. cine-camera.

A number of marker rings were placed along the tube and the ones to be used depended on the size and the rate of resorption of the particular bubble. Usually 7 markers were used for one bubble.

The manometer readings X_1 and X_2 were then taken and the experiment for one bubble was then complete. This was repeated for 4 or 5 more bubbles of different sizes.

The ambient pressure was then increased to start another experiment. At the end of a set of experiments for one particular air content the water in the tube was withdrawn and its air content again determined to see if any change had occurred during the experiment.

The cine film was developed at the end of all the experiments and the recorded times read with the help of a microscope.

3.5 Range covered by experiment

3.5.1 Ambient pressure

The ambient pressure of water was increased from atmospheric pressure to approximately 3 atmospheres (absolute), the maximum pressure available in the apparatus, in 3 steps.

3.5.2 Air content

Altogether 5 different air contents were investigated ranging from saturation to about 30% saturation.

3.5.3 Bubble Sizes

The maximum size of bubble investigated had a rising velocity of approximately 0.1 ft/sec which corresponds to a bubble of radius 5.6×10^{-4} ft (approx.).

Although bigger bubbles were also investigated but the rising velocities of these bubbles were too high for the change in velocities to be measured accurately with the present apparatus.

3.5.4 Temperature of Water

No attempt has been made in the present series of experiments to study the effect of temperature on the rate of resorption of air bubbles in water. The temperature of the tap water used in the experiment varied between 12° C and 15° C and a mean temperature of 13.5° C is used for all the calculations.

4. Experimental result

The complete experimental results are given in tables (1 to 5). Altogether about 120 bubbles were investigated but only 55 were chosen to be recorded and used in plotting the time-distance curves, since many are repetition results and others have too high a rising velocity for the decrease in velocity to be measured accurately.

A typical set of time-distance curves for these bubbles at one pressure setting and the same air content is shown in Fig (3). In fact these curves were plotted on a sheet of sectional paper of seven feet in length with the distance along the tube plotted full scale and time axis to the scale of 1 inch = 5sec. From the slopes of these curves the instantaneous rising velocities of bubbles at various positions along the main tube and under various experimental conditions were determined and tabulated in tables (6 to 10). By using the two sets of tables the rising velocity - time curves for individual bubbles can be plotted to determine the rate of decrease of rising velocity for various experimental conditions. Fig (4) shows a set of such curves for one air content but four different ambient pressures. Note that the curves are all straight lines and have the same slope for the same ambient pressure irrespective of the actual rising velocity of the bubble (i.e. independent of bubble sizes). The experimental results thus show that the rate of decrease of rising velocity ($\frac{dv}{dt}$) of a small air bubble in undersaturated water is constant

for one ambient pressure and is independent of the actual size of the bubble.

Table (11) contains the values of $\frac{dv}{dt}$ for the whole range of experimental conditions investigated.

In table (11) p_g is the air pressure inside the bubble, p_{X_3} is the ambient pressure of water in the main tube at a height of X_3 above the datum and p_L is the air content of water expressed in terms of equivalent saturation pressure by using Henry's Law.

p_{X_3} can be calculated from the manometer reading X_1 and X_2 and the atmospheric pressure p_b .

$$p_{X_3} = p_b + (X_2 - X_1) w_m - (X_3 - X_1) w_w \dots \dots \dots (4.1)$$

where w_m = density of mercury (lb/ft³)

w_w = density of water (lb/ft³)

The variation of pressure along the tube due to the variation of X_3 is small compared with other terms in equation (4.1) and it is assumed that p_{X_3} is constant along the tube and equal to the actual ambient pressure at the middle of the tube i.e., with $X_3 = 8.25$ ft (99 inches).

For a spherical gas bubble of radius r under an ambient pressure of p_{X_3} the gas pressure inside the bubble is given by equation,

$$p_g = p_{X_3} + \frac{2\sigma}{r} - p_v \dots \dots \dots (4.2)$$

where σ = surface tension (lb/ft)

p_v = vapour pressure of water (lb/ft²)

The term $\frac{2\sigma}{r}$ is negligible compare with other terms. The gas pressure inside the bubble is also assumed to be constant along the tube and equal to $(p_{X_3} - p_v)$. The values of p_{X_3} and p_g listed in table (11) are calculated from this simplified formula.

To determine the effects of various factors on the rate of decrease in rising velocities, $\frac{dv}{dt}$ is plotted as a function of p_g , $p_g - p_L$ and $1 - \frac{p_L}{p_g}$ (i.e. $1 - S$). The curves are shown in Fig (5,6&7).

From these curves it is clear that the rate of decrease in rising velocity for a small bubble in undersaturated water is not a sole function of p_g or $p_g - p_L$ but $1 - S$ (degree of undersaturation).

Since we have already observed in Fig (3) that $\frac{dv}{dt}$ is independent of bubble sizes, the experimental results thus point to the fact that $\frac{dv}{dt}$ is a linear function of $1 - S$ only.

The slope of the straight line in Fig (6) gives the empirical equation.

$$\begin{aligned} \frac{dv}{dt} &= -1.5 \times 10^{-3} (1-S) \\ &= -B_1 \times (1-S) \dots\dots\dots(4.3) \end{aligned}$$

where $B_1 = 1.5 \times 10^{-3}$

5. Analysis of Experimental results

5.1 Lewis-Whitman equation

To describe the resorption of air bubbles rising in tap water the Lewis-Whitman concept of gas and liquid films (ref 6) is adopted. The air bubbles concerned here are air bubbles which came out of solution and therefore contain approximately $\frac{1}{8}$ oxygen and $\frac{7}{8}$ nitrogen. Both of these gases are only slightly soluble in water. The equation to be used for the rate of transfer of gas per unit area is therefore the Lewis-Whitman equation for gases of low solubility (ref.6), since the gas film can be neglected in this case.

$$\text{i.e. } \frac{1}{A} \frac{dw}{dt} = -K_L (C_g - C_L) \dots\dots (5.1.1)$$

where w = weight of gas in bubble (lb)

A = interface area (ft²)

K_L = liquid coefficient (ft/sec)

C_g = concentration of gas in water saturated at a gas pressure p_g (lb/ft³)

when $C_g > C_L$, $\frac{dw}{dt}$ is negative and gas will diffuse out of the bubble into the water.

5.2 Rate of change of bubble radius

Consider a spherical gas bubble of radius r rising in undersaturated water under a constant temperature $T^{\circ}K$ and external pressure p_x . The gas pressure inside the bubble is given by equation (4.2)

$$P_g = P_{K_3} + \frac{2\sigma}{r} - F_v$$

The weight of gas inside the bubble is

$$w = \frac{4\pi r^3}{3} \frac{P_g}{RT} \dots\dots\dots(5.2.1)$$

where R = gas constant (ft³/K)

T = temperature of water (°K)

The rate of transfer of gas is therefore

$$\frac{dw}{dt} = 4\pi r^2 \frac{F_g}{RT} \frac{dr}{dt} \dots\dots\dots(5.2.2)$$

Since for a sphere A = 4πr².....(5.2.3)

$$\frac{1}{A} \frac{dw}{dt} = \frac{P_g}{RT} \frac{dr}{dt} \dots\dots\dots(5.2.4)$$

From equations (5.1.1) and (5.2.4) we have

$$\frac{dr}{dt} = -K_L (C_g - C_L) \frac{RT}{P_g} \dots\dots(5.2.5)$$

Henry's Law gives,

$$C = Hp \dots\dots\dots(5.2.6)$$

where H - Henry's constant (ft⁻¹)

Then we have

$$H = \frac{C_g}{P_g} = \frac{C_L}{P_L} \dots\dots\dots(5.2.7)$$

with equation (5.2.7) equation (5.2.5) becomes

$$\frac{dr}{dt} = -K_L HRT \left(1 - \frac{P_L}{P_g}\right)$$

i.e., $\frac{dr}{dt} = -K_L HRT (1 - S) \dots\dots\dots(5.2.8)$

where $S = \frac{P_L}{P_g} \dots\dots\dots(5.2.9)$

All the terms contained in equation (5.2.8) except K_L can be determined by experiments. Therefore equation (5.2.8) is to be used for evaluation K_L .

5.3 Bubble radius and its rising velocity

We now take the empirical equation (4.3)

$$\frac{dv}{dt} = -P_L (1 - S)$$

obtained from experiment on the one hand and the equation (5.2.8)

$$\frac{dr}{dt} = -K_L HRT (1 - S)$$

provided by the above analysis on the other.

To link these the relationship between the radius of a small air bubble and its rising velocity in tap water is determined.

Many experiments have been carried out in the past by various workers to determine the rising velocity of small air bubbles in various liquids. For example Allen (ref. 13) determines the rising

velocity of small air bubbles in water and in aniline. Arnold (ref.14) worked with air bubbles in olive oil and in aniline while Bond and Newton (ref.15) measured the rate of rising of air bubbles in Syrup and in waterglass.

But the most complete and recent work on the rising velocity of gas bubbles in various liquids is by Haberman and Morton (ref.16) which covers a wide range of bubble sizes and uses a large number of different liquids.

From their experimental results Haberman and Morton observed that the drag coefficient of air bubbles rising at their terminal velocities in tap water, filtered tap water and distilled water is equal to the drag coefficient of the corresponding rigid spheres for Reynolds numbers smaller than 40. Fig (8) is a reproduction of Fig (27) in reference (14) with the results for hot tap water omitted and that for Stokes Law inserted. They also observed that there is no significant difference between the rates of rise of bubbles composed of oxygen and of air.

It is therefore assumed that the drag coefficients of small air bubbles investigated in the present experiments in tap water at room temperature are equal to the drag coefficients of rigid spheres of the same diameters, since the largest bubble investigated in the present experiment has a Reynolds number 10.

Fig (9) shows the radius of bubble and its corresponding rising velocity in water at 13.5°C calculated from drag coefficient and Reynolds number for rigid spheres shown in Fig (8). For Reynolds number smaller than 0.5 the motion of the bubble is predicted by "Stokes' Law (ref.17), where the rising velocity is proportional to the square of the radius of bubble, while beyond the region where Stokes' Law is valid the rising velocity is a linear function of the radius of bubble.

For the convenience of calculation in evaluating the liquid coefficient K_L and the derivation of resorption equations it was decided to divide the relationship between the rising velocity and bubble radius into two separate regions, namely the Stokes' region and region beyond Stokes'.

Transition is assumed to take place at a rising velocity of 0.02 ft/sec as shown in Fig (9).

5.4 Evaluation of K_{L1}

Stoke's region

For the Stoke's region the rising velocity of air bubbles in water is given by equation.

$$v = \frac{2}{9} g \frac{\rho - \rho'}{\mu} r^2 \dots \dots \dots (5.4.1)$$

where g - gravitational acceleration (ft/sec²)

ρ - mass density of water (lbsec²/ft⁴)

ρ' - mass density of air in bubble (lbsec²/ft⁴)

μ - viscosity of water (lbsec/ft²)

On differentiating * (5.4.1)

$$\frac{dv}{dt} = \frac{4}{9} g \frac{\rho - \rho'}{\mu} r \frac{dr}{dt}$$

i.e., $\frac{dr}{dt} = B_2 \frac{1}{r} \frac{dv}{dt} \dots \dots \dots (5.4.2)$

where $B_2 = \frac{9}{4} \frac{\mu}{(\rho - \rho')g}$

substituting equation (4.3) and (5.2.8) into (5.4.2) we have

$$K_{L1} = \frac{B_1 B_2}{HRT} \frac{1}{r}$$

where K_{L1} denotes K_L for the Stoke's region.

i.e., $K_{L1} = B_3 \frac{1}{r} \dots \dots \dots (5.4.3)$

where $B_3 = \frac{B_1 B_2}{HRT} = 5.7 \times 10^{-8} \text{ft}^2/\text{sec}.$

Equation (5.4.3) shows that the value of K_L in the Stoke's region is independent of the ambient pressure or the air content of water but is inversely proportional to radius of the bubble.

Region beyond Stoke's

The rising velocity of air bubble in water is a linear function of the bubble radius as shown in Fig (7). The slope of the straight line is given by the equation

$$\begin{aligned} \frac{dv}{dr} &= \frac{dv}{dt} / \frac{dr}{dt} \\ &= 2.13 \times 10^2 \text{ sec}^{-1} \end{aligned}$$

i.e., $\frac{dr}{dt} = \frac{1}{2.13 \times 10^2} \frac{dv}{dt} \dots \dots \dots (5.4.4)$

Substituting equations (4.3) and (5.2.8) into (5.4.4)

we have, $K_{L2} = \frac{1}{2.13 \times 10^2} \times B_1 \times \frac{1}{HRT}$
 $= 3.0 \times 10^{-4} \text{ ft/sec}.$

* See appendix.

where K_{L2} denotes K_L in region outside Stoke's.

The liquid coefficient K_L is therefore a constant and equal to 3.0×10^{-4} ft/sec in the region beyond Stoke's and within the range of bubbles investigated in the experiment,

5.5 Resorption equations for air bubbles

With the value of liquid coefficient K_L determined it is now possible to derive the resorption equation for an air bubble in undersaturated water.

Brown (ref.5) derived a resorption equation for air bubbles under a constant ambient pressure equal to the mean pressure in the resorber, while Silverleaf(ref.4) considered the case of a continuously varying ambient pressure as well as the case of constant pressure. Both used a constant value of K_L for their analysis. Since for small air bubbles ($r < 2 \times 10^{-4}$ ft) the value of K_L is inversely proportional to the radius of the bubble a new analysis is provided to include this effect. The analysis with K_L equal to a constant value of 3.0×10^{-4} ft/sec (for bubble beyond the Stoke's region) is also included. This analysis is essentially the same as that of Silverleaf.

Resorption under varying ambient pressure

Consider an air bubble being transported down a vertical pipe of large diameter. The velocity of flow V is large compared with the rising velocity v of the bubble. At time $t = 0$ the bubble is located at position O . The radius of the bubble is r_0 and the ambient pressure is p_0 . At some later instant $t = t$ the bubble is at a new position S with radius r and ambient pressure p . Since the increase in ambient pressure is solely due to the increase in the hydrostatic head of water the pressure p at S is given by

$$p = p_0 + \rho g V t \dots \dots \dots (5.5.1)$$

The gas pressure inside the bubble is

$$p_g = p + \frac{2\sigma}{r} - P_v$$

Assume $\frac{2\sigma}{r}$ and p_v are small compared with p .

Therefore $p_g = p \dots \dots \dots (5.5.2)$

The weight of gas inside the bubble is

$$w = \frac{4}{3} \pi \frac{p}{RT} r^3$$

and $\frac{dw}{dt} = 4\pi r^2 \frac{1}{RT} \left[p \frac{dr}{dt} + \frac{1}{3} r \frac{dp}{dt} \right]$

For a sphere $A = 4\pi r^2$

i.e., $\frac{1}{A} \frac{dw}{dt} = \frac{1}{3RT} \left[3p \frac{dr}{dt} + r \frac{dp}{dt} \right] \dots \dots \dots (5.5.3)$

With equation (5.1.1), equation (5.5.3) becomes

$$\frac{1}{3RT} \left[3p \frac{dr}{dt} + r \frac{dp}{dt} \right] = -K_L (C_g - C_L) = -K_L H (p - p_L) \dots \dots \dots (5.5.4)$$

Since $H = \frac{C_g}{p} = \frac{C_L}{p_L}$

From equation (5.5.1)

$$\frac{dp}{dt} = \rho g v$$

and since

$$\frac{dr}{dp} = \frac{dr}{dt} / \frac{dp}{dt}$$

$$\frac{dr}{dt} = \rho g v \frac{dr}{dp} \dots \dots \dots (5.5.5)$$

Equation (5.5.4) is then,

$$3p \frac{dr}{dp} + r = - \frac{3HRT}{\rho g v} K_L (p - p_L) \dots \dots \dots (5.5.6)$$

For Stoke's region ($K_{L1} = B_3 \times \frac{1}{r}$)

Equation (5.5.6) becomes,

$$3pr \frac{dr}{dp} + r^2 = - \frac{3HRTB_3}{\rho g v} (p - p_L)$$

i.e., $3pr \frac{dr}{dp} + r^2 + B_4 (p - p_L) = 0 \dots \dots \dots (5.5.7)$

where

$$B_4 = \frac{3HRTB_3}{\rho g v} = \frac{3B_1B_2}{\rho g v}$$

The resorption equation is obtained by integrating

(5.5.7) and by putting $r = r_0$ at $p = p_0$

The equation is

$$r^2 = \left[r_0^2 + B_4 \left(\frac{2}{5} p_0 - p_L \right) \right] \left(\frac{p_0}{p} \right)^{2/3} - B_4 \left(\frac{2}{5} p - p_L \right) \dots \dots \dots (5.5.8)$$

Since $p = p_0 + \rho g v t$ (for increasing pressure).

Equation (5.5.8) becomes

$$r^2 = \left[r_0^2 + \frac{3B_1B_2}{\rho g v} \left(\frac{2}{5} p_0 - p_L \right) \right] \left(\frac{p_0}{p_0 + \rho g v t} \right)^{2/3}$$

$$- \frac{3B_1B_2}{\rho g v} \left[\left(\frac{2}{5} p_0 - p_L \right) + \frac{2}{5} \rho g v t \right] \dots \dots \dots (5.5.9)$$

For region beyond Stoke's ($K_{L2} = 3 \times 10^{-4}$ ft/sec)

The analysis is the same as that presented by Silverleaf (ref. 4) but is repeated here.

From equation (5.5.6)

$$3p \, dr + r \, dp + \frac{3HRT}{\rho g V} K_{L2} (p - p_L) \, dp = 0$$

i.e., $3p \, dr + r \, dp + B_5 (p - p_L) \, dp = 0 \dots \dots \dots (5.5.10)$

where $B_5 = \frac{3HRT}{\rho g V} K_{L2}$

By integrating (5.5.10) and putting $p = p_o$ for $r = r_o$, the resorption equation is obtained.

$$r = \left(\frac{p_o}{p}\right)^{1/3} \left[\frac{1}{4} B_5 p_o + (r_o - B_5 p_L) \right] - \frac{1}{4} B_5 p + B_5 p_L$$

Since $p = p_o + \rho g V t$ (for increasing pressure)

The resorption equation is then

$$r = \left(\frac{p_o}{p_o + \rho g V t}\right)^{1/3} \left[r_o + \frac{3HRT}{4\rho g V} K_{L2} (p_o - 4p_L) \right] - \frac{3HRT}{4\rho g V} K_{L2} (p_o - 4p_L) - \frac{3}{4} HRT K_{L2} t \dots \dots \dots (5.5.11)$$

For decreasing ambient pressure

$$p = p_o - \rho g V t$$

is used.

Resorption of air bubbles under constant ambient pressure

The resorption equation can be obtained directly from equation (5.2.8)

$$\frac{dr}{dt} = - K_L HRT (1 - S)$$

with p_g replaced by p , the constant ambient pressure.

For Stoke's region ($K_{L1} = B_3 \frac{1}{r}$)

$$\frac{dr}{dt} = - B_3 \frac{HRT}{r} (1 - S)$$

i.e., $rdr = HRT B_3 (1 - S) dt \dots \dots \dots (5.5.12)$

On integrating eqn (5.5.12) and by putting $r=r_0$ at $t=0$, the resorption equation is obtained in the form.

$$r^2 = r_0^2 - 2B_3 \text{HRT} (1-S) t$$

i.e., $r^2 = r_0^2 - 2B_1 B_2 (1-S) t \dots \dots \dots (5.5.13)$

Since $B_3 = \frac{B_1 B_2}{\text{HRT}}$

For the region beyond Stoke's ($K_{L2} = 3.0 \times 10^{-4}$ ft/sec).

Since K_{L2} is a constant, the resorption equation is obtained by integrating the equation (5.2.8) direct and letting $r = r_0$ for $t = 0$

The resorption equation is

$$r = r_0 - K_{L2} (1-S) \text{HRT} t \dots \dots \dots (5.5.14)$$

6. Sources of Errors.

Air content of water.

The measurement of the air content by using the M.E.R.L. air content apparatus (ref.10) and the corrections suggested by Kenellopoulos (ref.11 and 12) is thought to be within an accuracy of $\pm 1-2\%$. A possible source of error is the slight increase in air content due to the resorption of injected air bubbles. To determine the amount of increase in air content during an experiment measurements of air content are carried out before and after each set of experiments for each sample of water used. The maximum increase in air content recorded was $2\frac{1}{2}\%$.

Temperature of Water

The temperature of water used in the experiment was not controlled and depended on the room temperature which varied from 12°C to 15°C . For calculating the experimental results a mean temperature of 13.5°C is used throughout. This variation in temperature introduces error in two ways. Firstly the viscosity of water varies with temperature and the change in visicosity for a temperature difference of $\pm 1.5^\circ\text{C}$ at 13.5°C is $\pm 4\%$. The error involved in deriving the radius of air bubble from its rising velocity using a mean temperature of 13.5°C is approximately $\pm 2\%$ for bubbles inside the Stoke's region and $\pm 4\%$ for those outside it. Secondly there is evidence that K_L will increase with increasing temperature (ref 9).

Although there is no definite information on the variation of K_L with temperature for small air bubbles rising in undersaturated water, it is thought the error will be between $\pm 3-5\%$ for a temperature variation of $\pm 1.5^\circ\text{C}$.

Measurement of rising velocity of air bubble.

The accuracy of the rising velocity depends on the recording of the time and the determination of the slopes of the time-distance curves. The stop-watch used has a scale which allows time to be read to the accuracy of 0.1 sec. Little error is involved in the actual recording of the watch reading on film since with practice the time recorded will be within $\frac{1}{2}$ sec of the actual time. A more serious error may be introduced in determining the slope of the Time-distance curves. Although the curves were plotted full scale the slope may have a variation of up to 5% depending on the judgement of the person concerned.

Variation of hydrostatic pressure along the tube

In the analysis of experimental results it is assumed that the bubble is subjected to a constant ambient pressure equal to the mean ambient pressure in the tube. Since the hydrostatic pressure is higher at the bottom than the top part of the tube the error introduced in assuming a constant mean pressure is $\pm 5\%$ at atmospheric pressure and $\pm 3\%$ at the max available ambient pressure of approximately 3 atmospheres (absolute).

Wall effect

In deriving the radius of a small air bubble and its rising velocity in water the information contained in Fig (8) about the drag coefficient and Reynolds number for rigid spheres are used. Since this information only applies to rigid spheres moving in an infinite medium it is necessary to consider the effect of the container wall on the rising velocity of small air bubbles. The case of a rigid sphere moving in a stationary liquid inside a cylindrical tube has been solved theoretically by Haberman and Sayre (ref.18). The theoretically deduced correction factor for drag is given as a function of diameter ratio and agrees well with experimental results. This correction factor can be used in the present experiment to estimate the effect of container wall on the rising velocity of small air bubbles. The largest bubble

investigated has a radius $r = 5.6 \times 10^{-4}$ ft. Since the radius of the cylindrical tube used is 4.2×10^{-2} ft, the decrease in drag for an air bubble with $r = 5.6 \times 10^{-4}$ ft is 2% over that in a infinite medium resulting in a 2% reduction of the rising velocity for the same size of bubble.

7. Discussion

The evaluation of the liquid coefficient K_L in the present experiment is essentially empirical in nature. The derivation was based on the experimental result of bubbles. There is a certain amount of scatter in the final results. This is to be expected since the temperature of water was not controlled in the present experiment and also the determination of the rising velocities may well be subject to an error of $\pm 5\%$. An analytical determination of the slopes of the Time-Distance curves will certainly improve matters but it was felt that the effort would not be justified under the present experimental conditions. The variation in temperature alone would have introduced an error of $\pm 2 - 4\%$.

The most significant result of the experiment is the linear decrease in the rising velocity of small air bubbles with time in undersaturated water. This confirms the observation of Liebermann (ref.7)

However, there is a qualification to be made regarding the validity of the resorption equations for very small bubbles. In the experiment at least one small bubble was completely resorbed within the length of the main tube for each set of experimental conditions. The bubble was observed to disappear completely, but the time at which this happened was not recorded, since the visibility of the bubble depended on the lighting arrangement and there was always some doubt as to the precise moment at which the bubble disappeared. The lowest rising velocity recorded in the experiment was approximately 1×10^{-2} ft/sec corresponding to a bubble of radius $r = 1.3 \times 10^{-4}$ ft. Since no end points were obtained it was assumed that the linearity of the decrease in rising velocity also applied to bubbles with radius smaller than 1.3×10^{-4} ft. There is some experimental evidence that contamination in water sometimes delayed the complete resorption of very small air bubbles.

If this happens the resorption equations obtained for the Stoke's region will underestimate the time required for the complete resorption of very small bubbles.

8. Conclusions.

(1) The rate of decrease of rising velocity of small air* bubbles ($r < 5.6 \times 10^{-4}$ ft, the maximum size investigated) in undersaturated water is independent of actual bubble size but is a linear function of the degree of undersaturation ($1 - S$) at a constant water temperature.

(2) At a water temperature of 13.5°C the value of the empirical liquid coefficient K_L for small air bubbles rising in undisturbed undersaturated tap water depends on the radius of the bubble. For bubbles whose motion are correctly predicted by Stoke's Law ($r < 2.0 \times 10^{-4}$ ft) K_L is inversely proportional to the radius of the bubble and equal to $5.7 \times 10^{-8} \times \frac{1}{r}$ ft/sec. For bigger bubbles (2.0×10^{-4} ft $< r < 5.6 \times 10^{-4}$ ft) K_L is a constant and equal to 3.0×10^{-4} ft/sec. The largest bubble investigated in the present experiment had a radius $r < 5.6 \times 10^{-4}$ ft/sec.

(3) The value of K_L obtained in the present experiment can be used to estimate the minimum time required for the resorption of an air bubble of a certain size and to determine the maximum physical dimensions of the resorber for the complete resorption of air bubbles of given initial sizes.

The resorption equations for a constant and continuously varying external pressure are derived and listed as equations (5.5.9), (5.5.11), (5.5.13) and (5.5.14). The validity of the resorption equations for bubbles in the Stoke's region is subjected to the qualification stated in section (7).

- - - - -

* Air = $\frac{1}{5}$ oxygen + $\frac{4}{5}$ nitrogen.

REFERENCES

- (1) Knapp, R.T., Levy, J., O'Neill, J.P. Brown, F.B.
"The Hydrodynamic Laboratory of the California Institute of Technology." Trans. Amer. Soc. Mech. Engrs. 70, 1948.
p. 437.
- (2) Lever, E.H., Ritter, H., Woolfson, M., & Wright, C.T.
"The Rotating Beam Channel and 30 inch Water Tunnel at Admiralty Research Laboratory." Proc. Instn. Mech. Engrs., 171, 1957.
- (3) Hutton, S.F.
"Techniques for Hydraulic Machinery Research" Trans. Inst. E. & S. Scotland, 100, p. 351, 1956 - 7.
- (4) Silverleaf, A.
"The design of a resorber for a water tunnel" N.P.L. Ship Division Report No. 1, 1958.
- (5) Brown, F. Barton
"Air resorption in water tunnels" Hydrodynamics Laboratory, Calif. Inst. Tech., Report N-62. 1949.
- (6) Lewis, W.K. & Whitman, W.G.
"Principle of gas absorption" Ind. Eng. Chem. 16, p.p. 12/2 - 20, 1924.
- (7) Sillerman, E.
"Air bubble resorption" St. Anthony Falls Hydraulic Laboratory Tech. paper No. 1, Series B, 1949.
- (8) Hutchinson, M.H. & Sherwood, T.K.
"Liquid film in gas absorption" Ind. Eng. Chem. 29, p.p. 836 - 40, 1937.
- (9) Liebermann, L.
"Air bubbles in water" Jl. of Appl. Phys. 28, 2, p. 205, 1957.

- (10) McNulty P.J.
"The M.E.R.L. gas content apparatus" Mechanical Engineering
Research Laboratory Fluids Memo No. 35, 1955.
- (11) Kanellopoulos, E.V.
"New method for measuring the gas content of water"
Mechanical Engineering Research Laboratory Fluids Report
No. 69, 1958.
- (12) Kanellopoulos, E.V.
"Errors in measuring the gas content of water" Mechanical
Engineering Research Laboratory Fluid Report No. 73, 1958.
- (13) Allen, H.S.
"The motion of a sphere in a viscous fluid" Phil. Mag.,
1900, vol. 50, pp. 323 - 338, 519 - 534.
- (14) Arnold, H.D.
"Limitations imposed by slip and inertia terms upon
Stoke's Law for the motion of spheres through liquids"
Phil. Mag., 1911, vol. 22, pp. 755 - 775.
- (15) Bond, W.N., & Newton, Dorothy A.
"Bubbles, drops and Stoke's law " Phil. Mag. 1928,
vol. 5, pp. 794 - 800.
- (16) Haberman, W.L., & Morton, R.F.
"An experimental investigation of the drag and shape of
air bubbles rising in various liquids" David Taylor
Model Basin Report 802, 1953.
- (17) Stoke
Math and Phys. paper 2, 10, 1880.
- (18) Haberman, W.L., & Sayre, R.M.
"Motion of rigid and fluid spheres in stationary and
moving liquid inside cylindrical tubes" David Taylor
Model Basin Report 1143, 1958.
- (19) Duncan, W.J.
Private communication.

Appendix

For an air bubble rising in undersaturated water the forces acting on the bubble can be approximately expressed in the following form.

$$D + D_I - B = Ma \dots \dots \dots (1)$$

where D - drag of bubble of radius r

D_I - induced drag due to the change in bubble radius as air diffuses out of the bubble.

B - buoyancy force of bubble.

M - mass of the air bubble.

A - acceleration of the air bubble.

For an air bubble rising at terminal velocity $D_I = a = 0$ and equation (1) becomes.

$$D - B = 0 \dots \dots \dots (2)$$

In carrying out the differentiation of equation (5.4.1) it was necessary to assume that the terms D_I and Ma were insignificant and equation (2) was sufficient in expressing the motion of an air bubble rising in undersaturated water.

To justify the above assumption two numerical examples are worked out.

(1) Value of Ma

The largest bubble used in the experiment has a radius $r = 5.6 \times 10^{-4}$ ft and the highest value of a is equal to 0.0013 ft/sec². Under the maximum ambient pressure $p = 4800$ lb/ft² the mass of gas inside the bubble,

$$M = \frac{p}{RTg} \frac{4}{3} \pi r^3 \dots \dots \dots (3)$$
$$= 3.96 \times 10^{-12} \text{ lb sec}^2/\text{ft}$$

Therefore

$$Ma = 5.2 \times 10^{-15} \text{ lb}$$

(2) Value of D_I

The drag induced for a slow moving sphere with a decreasing radius in a perfect fluid is given by Duncan

(ref 19) as

$$D_I = \frac{1}{2} \times 4\pi r^2 \frac{dr}{dt} \times \rho \times v \dots \dots \dots (4)$$

With $r = 5.6 \times 10^{-4}$ ft the corresponding rising velocity $v = 1.0 \times 10^{-2}$ ft/sec.

Since

$$\frac{dr}{dt} = \frac{dv}{dt} / \frac{dv}{dr}$$

and $\frac{dv}{dt} = a = 0.0013$ ft/sec²

$$\frac{dv}{dr} = 2.13 \times 10^2 \quad \text{from (Fig 9)}$$

Therefore

$$\left(\frac{dr}{dt}\right)_{\text{Max}} = 6.15 \times 10^{-6} \text{ ft/sec}$$

Hence from equation (4)

$$D_I = 7.1 \times 10^{-11} \text{ lb}$$

For an air bubble in water of radius

$$r = 5.6 \times 10^{-4} \text{ ft}$$

the boyancy force

$$\begin{aligned} B &= \frac{4}{3} r^3 \times w_w \\ &= 3.27 \times 10^{-8} \text{ lb} \end{aligned}$$

Therefore

$$\frac{M_a}{B} = 1.6 \times 10^{-7}$$

and $\frac{D_I}{B} = 2 \times 10^{-3}$

It was thus considered justified to assume that equation (2) is adequate to express the motion of a small air bubble rising in undersaturated water.

LIST OF TABLES AND FIGURES

TABLES

1. to 5. Time-Distance record
6. to 10. Velocity-Distance record
11. Summary of Experimental results

FIGURES

1. Detail drawing of apparatus
2. Cine-camera arrangement
3. Time-Distance curve
4. Rising velocity of bubble-Time curve
5. Effect of p_g on $\frac{dv}{dt}$
6. Effect of $p_g - p_L$ on $\frac{dv}{dt}$
7. Effect of undersaturation on $\frac{dv}{dt}$
8. Drag coefficient as a function of Reynolds number for air bubbles rising at their terminal velocities in tap water.
9. Terminal velocity of air bubble in tap water as a function of bubble radius.

P_{x3} (MEAN) LB/FT ²	EXPERIMENTAL NUMBER	$P_L = 2.175 \text{ LB/FT}^2$ $P_b = 2.140 \text{ LB/FT}^2$ $T = 14.6^\circ\text{C}$																		
		X_3 IN INCHES																		
		69	76	81	87	89	93	95	97	100	101.5	103	105	108	111	114	117	123	129	
		TIME IN SECONDS																		
2850	6-2-3	0		12.2			25.0						38.9				53.4	60.9	68.9	
"	6-2-6	0		15.1			32.2						51.5				73.5	86.1	99.9	
"	6-2-1	0	18.8	36.8	78.2															
3760	6-3-2	0		9.7			19.9						30.7				42.5	48.8	55.2	
"	6-3-4	0		11.9			25.1						40.1				57.5	67.9	80.2	
"	6-3-1	0		23.2	40.0	47.4	75.5						29.7				41.6	47.3	55.8	
5240	6-4-6	0		9.1			18.8						33.6				48.8	57.6	68.1	
"	6-4-4	0		10.0			21.2						54.9	64.5	80.6					
"	6-4-2	0		13.4			30.3													

TABLE-1 TIME - DISTANCE RECORD

P_{x_3} (MEAN) LB/FT ²	EXPERIMENTAL NUMBER	$P_L = 1710$ LB/FT ² $P_b = 2145$ LB/FT ² $T = 14.2^\circ\text{C}$																	
		X_3 IN INCHES																	
		69	76	81	87	89	93	95	97	100	101.5	103	105	108	111	114	117	123	129
		TIME IN SECONDS																	
2080	3-1-1	0		15.1			31.7							49.2			68.0	77.7	88.0
"	3-1-2	0		26.1	41.5		60.0		87.4			102.5	115.0	141.6					
2980	3-2-3	0		11.4			23.7							37.9			52.6		73.2
"	3-2-4	0		12.0			25.5							41.0			59.4	70.7	84.1
"	3-2-2	0		15.3			34.2		48.5					61.0	70.4	83.5			
4040	3-3-4	0		9.0			19.3							30.5			42.9	50.3	58.1
"	3-3-5	0		10.3			22.3							35.8			52.5	62.7	75.6
"	3-3-2	0		17.8	29.7		46.5	55.7											
5360	3-4-4	0		8.9			18.4							29.1			41.3	48.2	55.6
"	3-4-1	0		9.6			20.4							32.8			48.1	57.6	69.9
"	3-4-3	0		15.0	24.5		36.0		47.0	59.1									

TABLE-2 TIME - DISTANCE RECORD

P_3 (MEAN) LB/FT ²	EXPERIMENTAL NUMBER	$P_L = 1380 \text{ LB/FT}^2$ $P_b = 2160 \text{ LB/FT}^2$ $T = 12.9^\circ\text{C}$																	
		X_3 IN INCHES																	
		69	76	81	87	89	93	95	97	100	101.5	103	105	108	111	114	117	123	129
		TIME IN SECONDS																	
2305	4-1-7	0	8.4				17.0						26.0			35.0	39.7	44.7	
"	4-1-3	0	12.6				27.4						44.3			65.7	79.3	97.0	
"	4-1-4	0	14.9	23.4			32.4			44.9			56.4		70.7	80.5	93.4		
3155	4-2-5	0	11.8				24.5			33.9			41.2		50.8	62.4			78.3
"	4-2-6	0	13.4				29.8			41.7			52.7	60.2	70.7	88.2			
4030	4-3-7	0	9.5				20.1						30.1			44.4	52.9	62.8	
"	4-3-1	0	10.3				22.0						35.5			53.2	64.8	82.9	
"	4-3-5	0	11.8	22.6	43.4														
5310	4-4-4	0	7.0				14.2						21.9			30.0	34.5	39.0	
"	4-4-2	0	11.0				24.5			54.2			43.0		54.5	62.7	75.4		
"	4-4-5	0	13.8				31.5			47.2			69.5		57.4				

TABLE -3 TIME - DISTANCE RECORD

P_x (MEAN) LB/FT ²	EXPERIMENTAL NUMBER	$P_L = 1100$ LB/FT ² $P_B = 2150$ LB/FT ² $T = 13.2^\circ\text{C}$																	
		76	81	87	89	93	95	97	100	101.5	103	105	108	111	114	117	123	129	
		X_3 IN INCHES																	
		TIME IN SECONDS																	
2170	5-1-1	0	9.3			19.2								30.1			41.6	47.8	54.4
"	5-1-2	0	13.6			29.9		41.2						51.0	57.9	66.5	76.9	95.8	
"	5-1-3	0	9.8	28.8		43.4		58.0											
2950	5-2-6	0	8.7			17.8							27.9				38.9	44.8	51.6
"	5-2-5	0	10.4			21.6							42.0				50.3	57.7	71.8
"	5-2-4	0	12.8			27.9							65.1	79.9					
3890	5-3-4	0	8.6			17.9							28.2				39.9	46.6	53.9
"	5-3-1	0	12.6			27.9							51.5	61.3					
"	5-3-6	0	14.7			34.4		44.8	56.0	66.3									
5270	5-4-2	0	9.2			19.8							32.4				48.4	59.3	76.1
"	5-4-7	0	13.2		24.7	31.8		40.9	50.8	58.4									
"	5-4-4	0	15.4		29.8	40.5	48.9												

TABLE - 4 TIME - DISTANCE RECORD

P_x (MEAN) LB/FT ²	EXPERIMENTAL NUMBER	$P_L = 770 \text{ LB/FT}^2$ $P_b = 2135 \text{ LB/FT}^2$ $T = 13.6^\circ\text{C}$																	
		X_3 IN INCHES																	
		69	76	81	87	89	93	95	97	100	101.5	103	105	108	111	114	117	123	129
		TIME IN SECONDS																	
2305	2-1-2	0		9.5			19.7						31.8				45.7		63.5
"	2-1-1	0		12.1			26.3						45.5			69.1	88.2		
"	2-1-8	0		15.5	25.6		39.6		55.9										
3200	2-2-4	0		9.3			19.5						30.9				45.0	53.5	64.1
"	2-2-3	0		11.6			26.3						40.8	55.0	67.0				
"	2-2-6	0		13.4			31.8		40.3	49.4	55.9	67.2							
4140	2-3-4	0		8.2			17.2						27.6				39.4		54.4
"	2-3-5	0		9.8			20.7						34.4			47.6	53.4	69.4	
"	2-3-3	0		11.8			26.8			38.8			50.9	64.2					
4820	2-4-4	0		7.9			16.3						25.6				36.0		48.3
"		0																	
"	2-4-2	0		13.4	22.1		33.2		44.0	61.2									

TABLE - 5 TIME - DISTANCE RECORD

EXPERIMENTAL NUMBER	X ₃ IN INCHES																		
	69	76	81	87	89	93	95	97	100	101.5	103	105	108	111	114	117	123	129	
RISING VELOCITY OF BUBBLE <i>v</i> IN FT/SEC X 10																			
6-2-3	0.83		0.79			0.73						0.71				0.69		0.64	
6-2-6	0.67		0.62			0.54						0.48						0.34	
6-2-1	0.37	0.27	0.20	0.06															
6-3-2			0.98			0.94						0.89				0.83	0.79	0.76	
6-3-4	0.85		0.79			0.69						0.64				0.49		0.38	
6-3-1	0.53		0.34	0.25		0.06													
6-4-6	1.11		1.04			0.89										0.76		0.67	
6-4-4	0.98		0.95			0.85						0.73				0.62		0.47	
6-4-2	0.79		0.63			0.52						0.32	0.22	0.12					

TABLE-6 VELOCITY-DISTANCE RECORD

EXPERIMENTAL NUMBER	X ₃ IN INCHES																		
	69	76	81	87	89	93	95	97	100	101.5	103	105	108	111	114	117	123	129	
	RISING VELOCITY OF BUBBLE V ² IN FT/SEC X 10																		
3-1-1	0.67		0.63			0.59						0.56				0.52			0.48
3-1-2	0.41		0.34	0.30		0.25		0.18				0.13							
3-2-3	0.73		0.70			0.59						0.51				0.48			0.34
3-2-4	0.85		0.79			0.69						0.62							0.35
3-2-2	0.67		0.61			0.44						0.29	0.23	0.16					
3-3-4	1.11		1.01			0.90						0.83				0.74			0.61
3-3-5	0.98		0.95			0.79						0.67				0.53			0.35
3-3-2			0.48	0.39		0.22	0.15												
3-4-4	1.19		1.11			0.98						0.88				0.74	0.69		0.62
3-4-1	1.04		0.95			0.83						0.74				0.59			0.36
3-4-1	0.69		0.60	0.48		0.37		0.26	0.13										

TABLE-7 VELOCITY DISTANCE RECORD

EXPERIMENTAL NUMBER		X ₃ IN INCHES																	
		69	76	81	87	89	93	95	97	100	101.5	103	105	108	111	114	117	123	129
		RISING VELOCITY OF BUBBLE V IN FT/SEC X 10																	
4-1-7						1.19						1.11				1.04			0.98
4-1-3	0.85		0.73			0.64						0.53				0.41			0.25
4-1-4	0.73		0.62			0.52			0.44			0.37		0.28		0.23			0.17
4-2-5	0.88		0.83			0.69			0.60			0.56		0.48		0.38			0.25
4-2-6	0.76		0.67			0.54			0.43			0.36	0.28	0.19	0.11				
4-3-7	1.11		1.04			0.93						0.83				0.68			0.48
4-3-1	0.98		0.93			0.82						0.67				0.49	0.36		0.21
4-3-5	0.53	0.44	0.33	0.16															
4-4-4			1.39			1.33						1.28				1.19	1.14		1.11
4-4-2	0.95		0.83			0.67								0.35		0.14			
4-4-5	0.73		0.69			0.48			0.32			0.18	0.10						

TABLE 8 - VELOCITY-DISTANCE RECORD

EXPERIMENTAL NUMBER	X ₃ IN INCHES																		
	69	76	81	87	89	93	95	97	100	101.5	103	105	108	111	114	117	123	129	
	RISING VELOCITY OF BUBBLE V IN FT/SEC X 10																		
5-1-1	1.11		1.04			0.98						0.93				0.88		0.76	
5-1-2	0.73		0.67			0.58						0.38	0.33		0.19			0.08	
5-1-3	0.61		0.48	0.40		0.29	0.16												
5-2-6	1.19		1.15			1.04						0.95				0.86		0.69	
5-2-5			0.93			0.83						0.61				0.57		0.37	
5-2-4	0.79		0.76			0.59						0.38		0.23	0.12				
5-3-4	1.23		1.11			0.98						0.93				0.75		0.67	
5-3-1	0.83		0.75			0.59						0.31	0.22						
5-3-6	0.67		0.62			0.37		0.28	0.17	0.09									
5-4-2	1.11		0.98			0.86						0.74				0.52	0.40	0.23	
5-4-7	0.83		0.67		0.51	0.44		0.32	0.20	0.13									
5-4-4	0.73		0.56		0.39	0.27	0.16												

TABLE - 9 VELOCITY-DISTANCE RECORD

EXPT. NO.	\bar{p}_{x_3} (MEAN) LB/FT ²	p_g LB/FT ²	$p_g - p_L$ LB/FT ²	$i - g$	$\frac{dv}{dt} \times 10^4$ FT/SEC ²
6-2	2850	2817	672	.25	-3.6
6-3	3760	3727	1552	.42	-6.0
6-4	5240	5207	3032	.51	-8.3
$p_L = 2175$ LB/FT ²					
3-1	2080	2047	337	.17	-2.2
3-2	2980	2949	1237	.42	-5.9
3-3	4040	4007	2297	.58	-8.3
3-4	5360	5327	3617	.68	-9.6
$p_L = 1710$ LB/FT ²					
4-1	2305	2272	892	.40	-5.9
4-2	3155	3122	1742	.56	-8.3
4-3	4030	3997	2612	.66	-9.4
4-4	5310	5277	3897	.73	-10.6
$p_L = 1380$ LB/FT ²					
5-1	2170	2137	1037	.49	-7.6
5-2	2950	2917	1817	.62	-9.4
5-3	3890	3857	2757	.72	-10.6
5-4	5270	5237	4137	.79	-11.8
$p_L = 1100$ LB/FT ²					
2-1	2305	2272	1502	.65	-10.0
2-2	3200	3167	2397	.76	-11.5
2-3	4140	4107	3337	.81	-12.3
2-4	4820	4787	4017	.84	-13.1
$p_L = 770$ LB/FT ²					

TABLE - 11 SUMMARY OF EXPERIMENTAL RESULTS

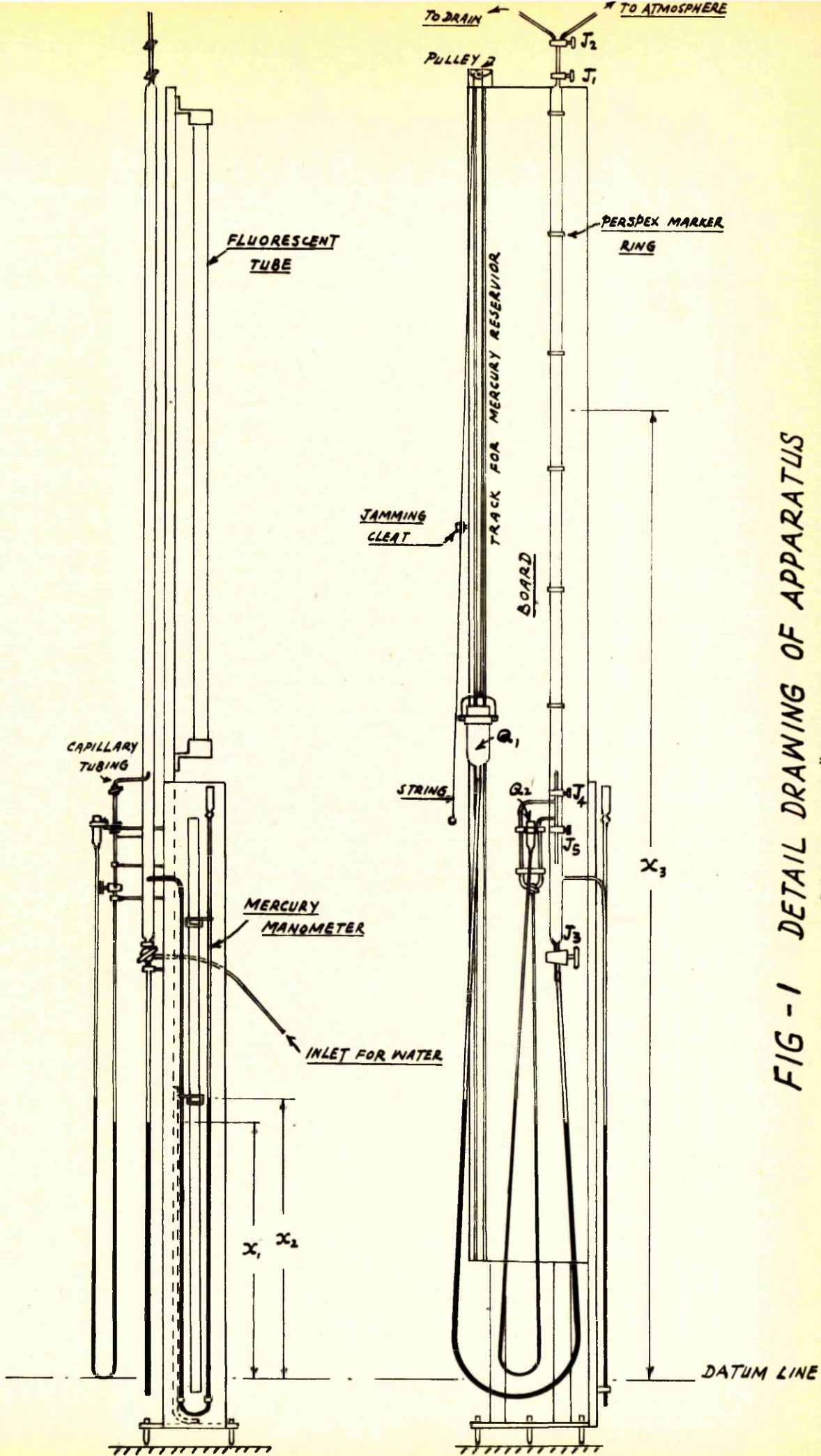


FIG - 1
 DETAIL DRAWING OF APPARATUS
 SCALE 1" = 1 FOOT

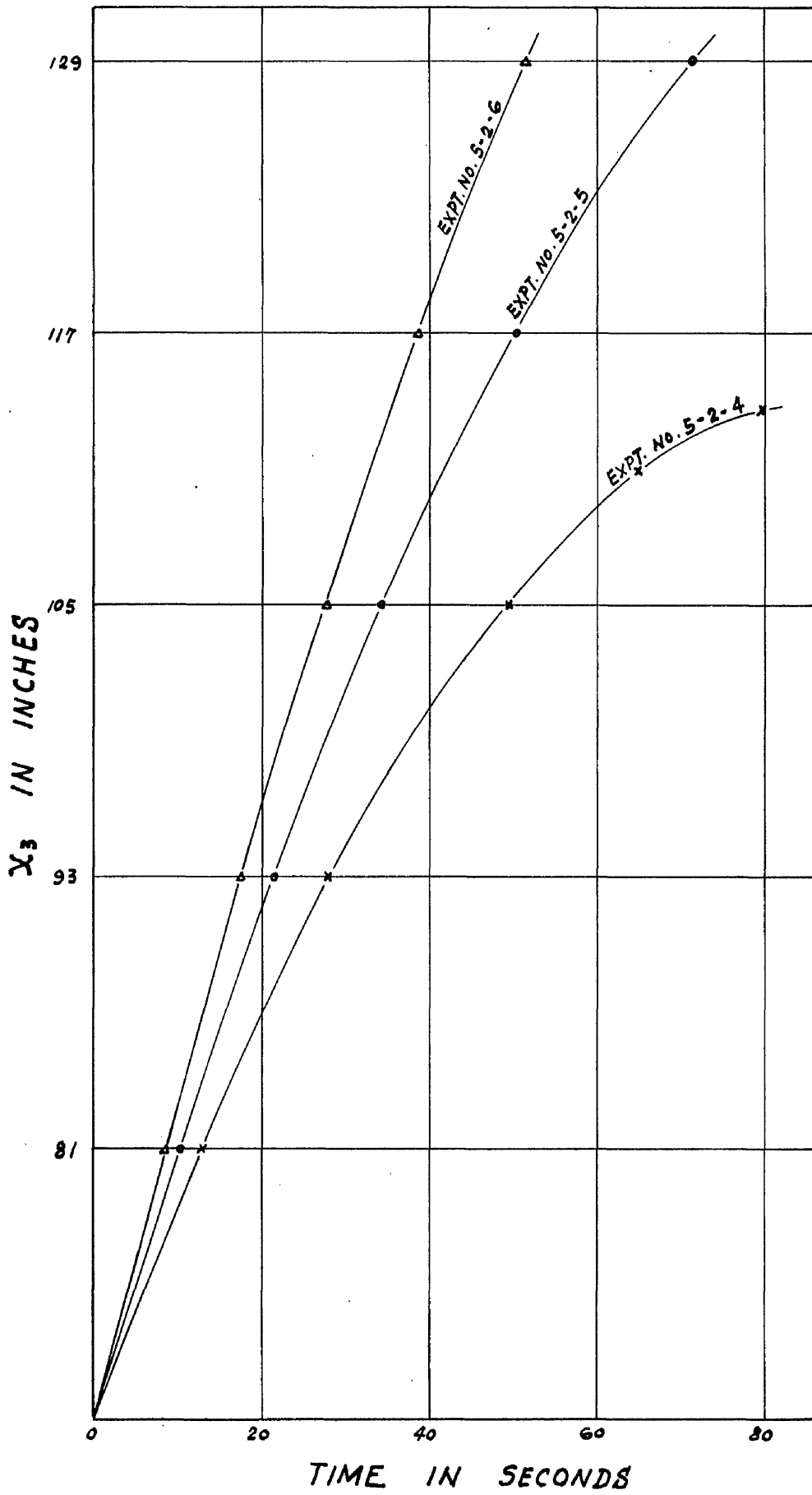


FIG - 3 TIME-DISTANCE CURVE

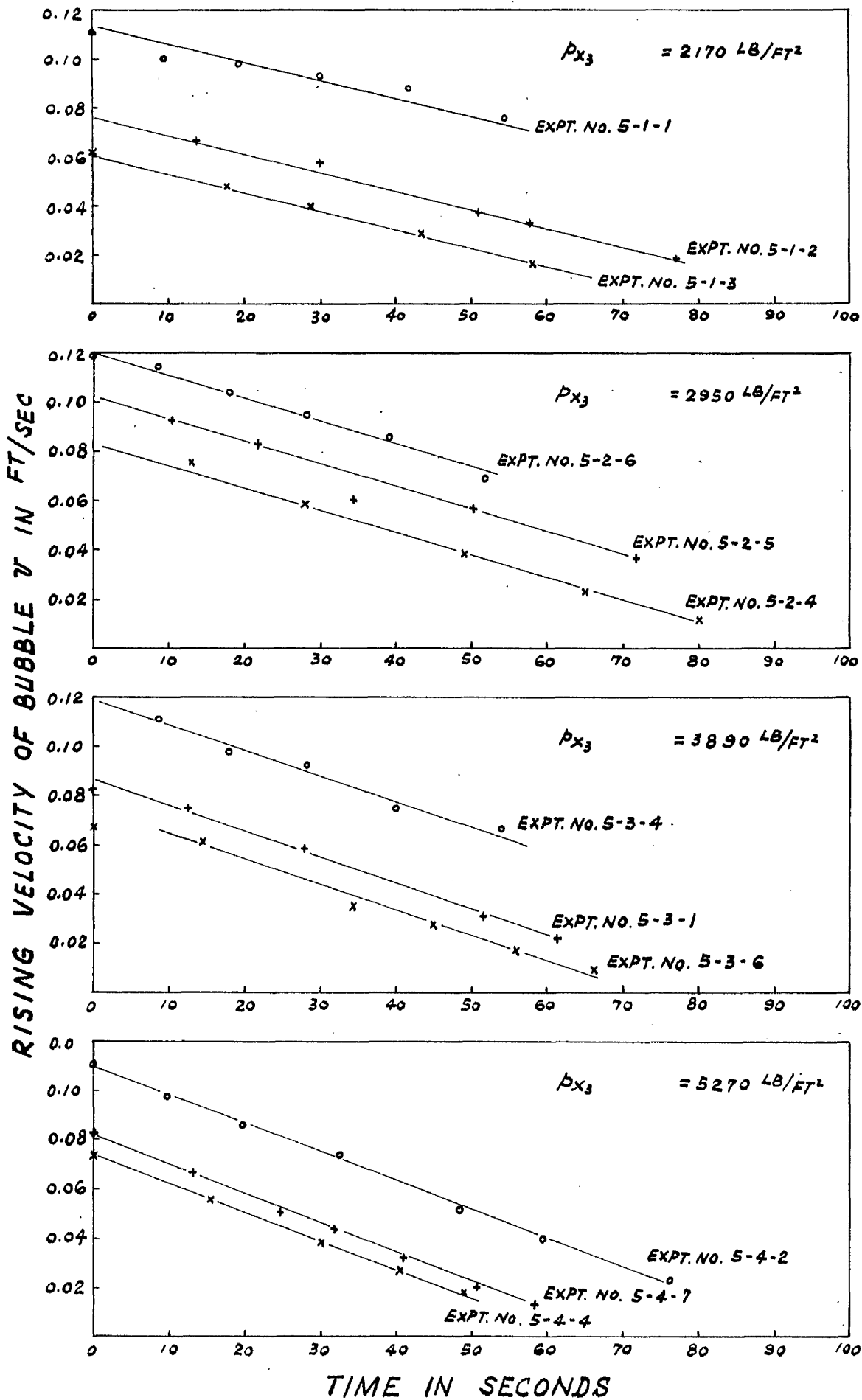


FIG 4 RISING VELOCITY OF BUBBLE-TIME CURVE

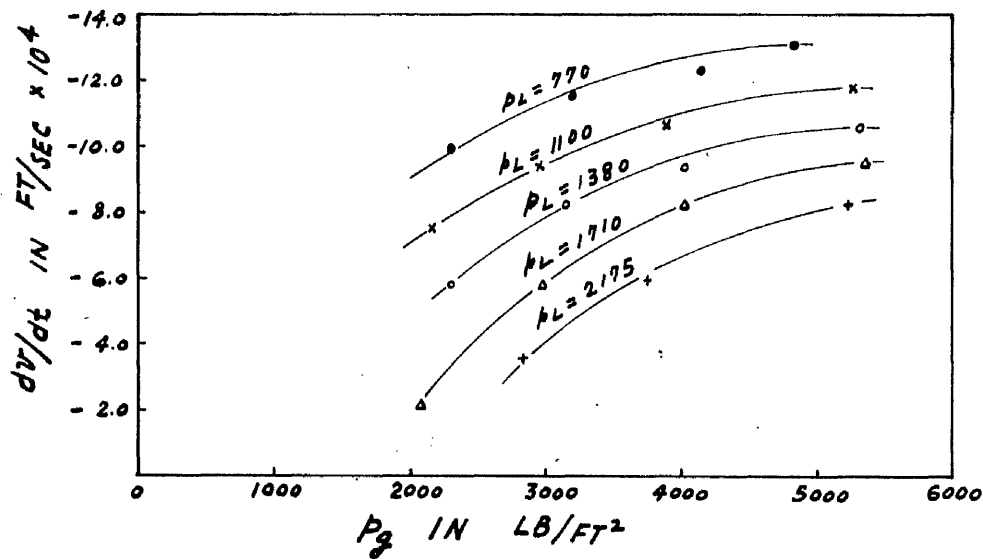


FIG 5 EFFECT OF P_g ON $\frac{dv}{dt}$

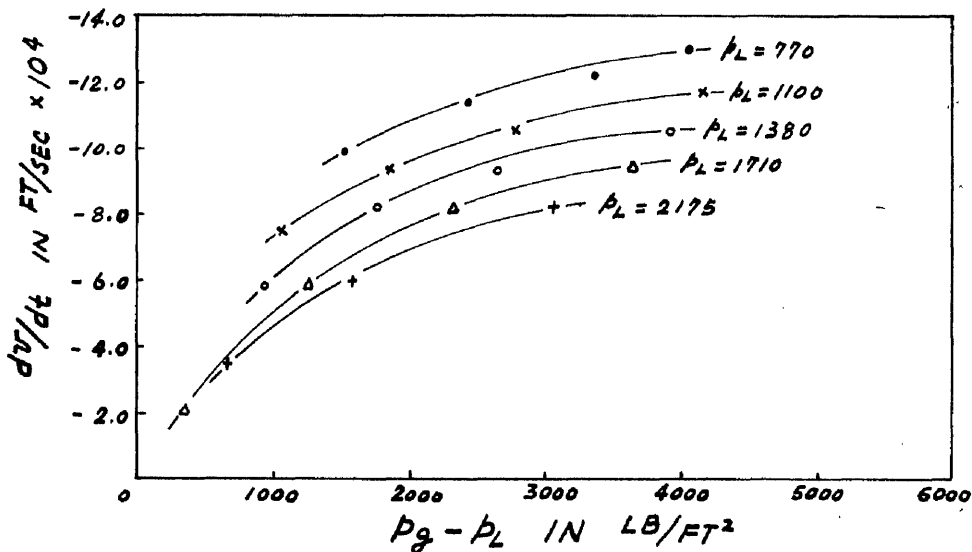


FIG 6 EFFECT OF $P_g - P_L$ ON $\frac{dv}{dt}$

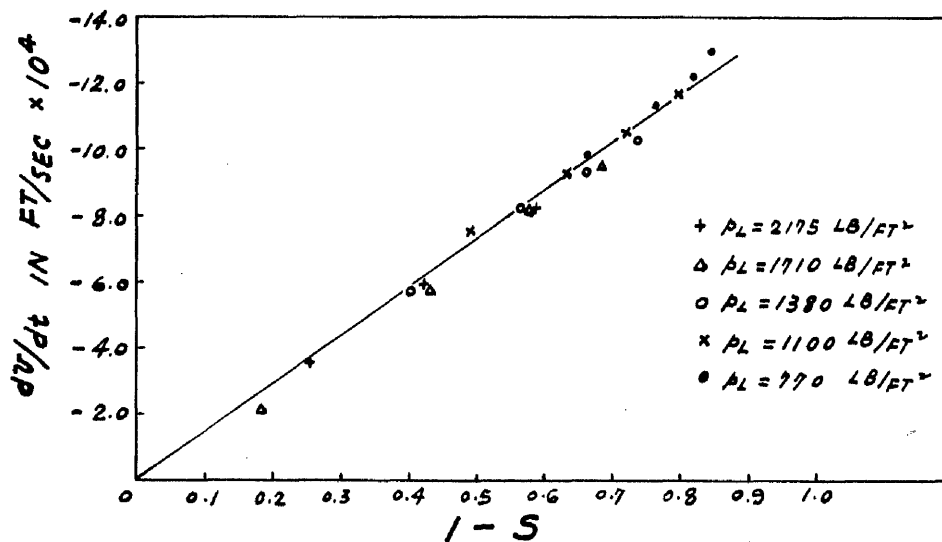


FIG 7 EFFECT OF UNDERSATURATION ON $\frac{dv}{dt}$

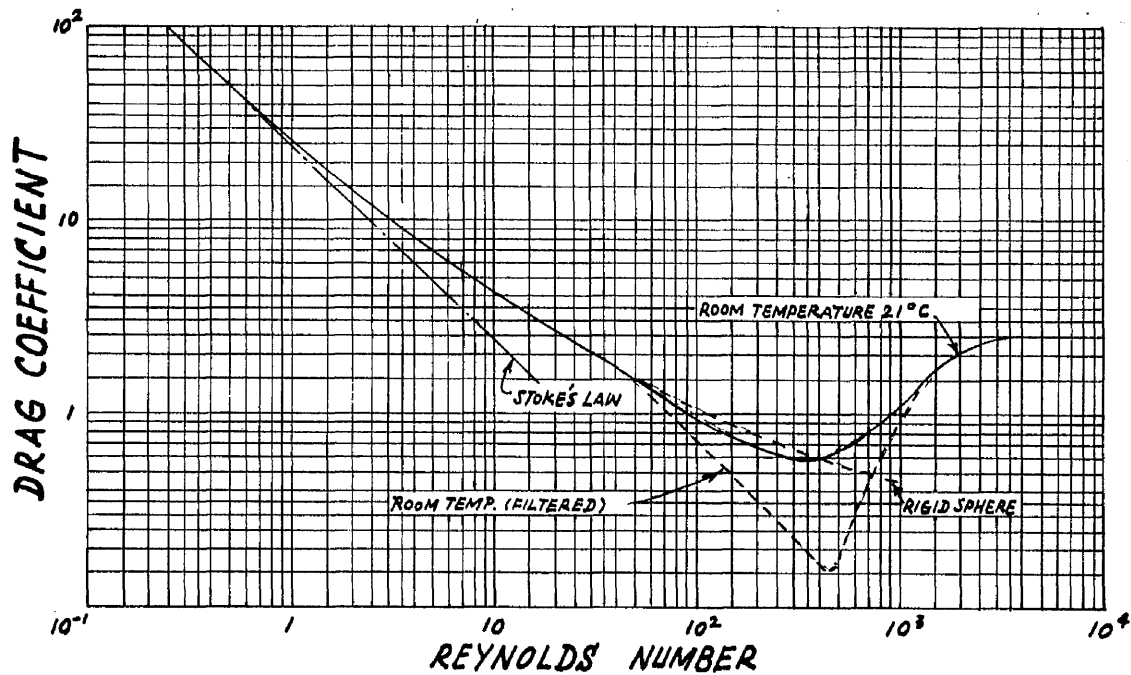


FIG 8 DRAG COEFFICIENT AS A FUNCTION OF REYNOLDS NUMBER FOR AIR BUBBLES RISING AT THEIR TERMINAL VELOCITY IN TAP WATER

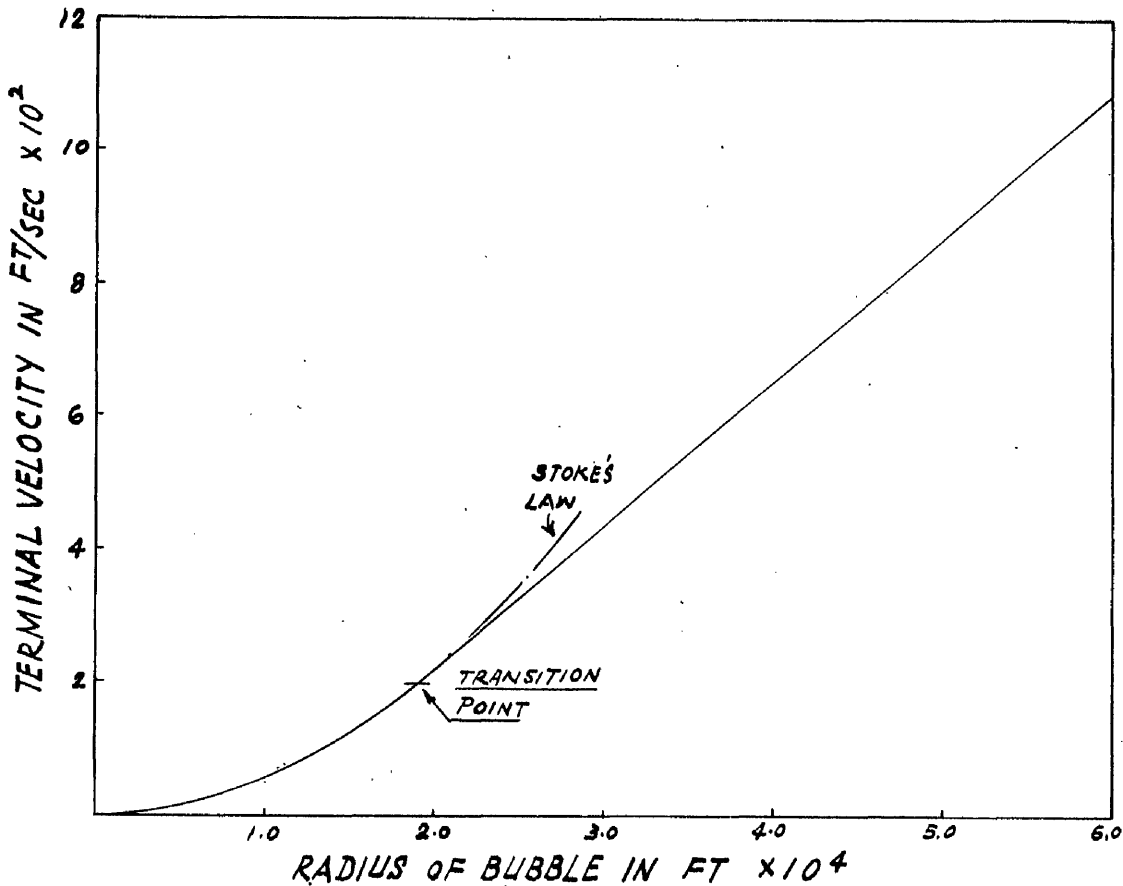


FIG 9 TERMINAL VELOCITY OF AIR BUBBLE IN TAP WATER AS A FUNCTION OF BUBBLE RADIUS

